NAVAL POSTGRADUATE SCHOOL
Monterey, California

THESIS

COMPUTER-CONTROLLED PHOTODETECTOR CHARACTERIZATION SYSTEM (DESIGN AND CONSTRUCTION)

by

Bryan E. Herdlick

December 2002

Thesis Advisor:	Gamani Karunasiri
Second Reader:	Scott Davis

Approved for public release; distribution is unlimited.

THIS PAGE INTENTIONALLY LEFT BLANK

REPORT DOCUMENTATION PAGE			*Form Approved OMB No. 0704-0188*
Public reporting burden for this collection of information is estimated to average 1 hour per response, including the time for reviewing instruction, searching existing data sources, gathering and maintaining the data needed, and completing and reviewing the collection of information. Send comments regarding this burden estimate or any other aspect of this collection of information, including suggestions for reducing this burden, to Washington headquarters Services, Directorate for Information Operations and Reports, 1215 Jefferson Davis Highway, Suite 1204, Arlington, VA 22202-4302, and to the Office of Management and Budget, Paperwork Reduction Project (0704-0188) Washington DC 20503.			
1. AGENCY USE ONLY *(Leave blank)*	**2. REPORT DATE** December 2002	**3. REPORT TYPE AND DATES COVERED** Master's Thesis	
4. TITLE AND SUBTITLE: Computer Controlled Photodetector Characterization System (Design and Construction)			**5. FUNDING NUMBERS**
6. AUTHOR(S) Bryan E. Herdlick, LCDR, USN			
7. PERFORMING ORGANIZATION NAME(S) AND ADDRESS(ES) Naval Postgraduate School Monterey, CA 93943-5000			**8. PERFORMING ORGANIZATION REPORT NUMBER**
9. SPONSORING /MONITORING AGENCY NAME(S) AND ADDRESS(ES) N/A			**10. SPONSORING/MONITORING AGENCY REPORT NUMBER**
11. SUPPLEMENTARY NOTES The views expressed in this thesis are those of the author and do not reflect the official policy or position of the Department of Defense or the U.S. Government.			
12a. DISTRIBUTION / AVAILABILITY STATEMENT Approved for public release; distribution is unlimited.			**12b. DISTRIBUTION CODE** A
13. ABSTRACT *(maximum 200 words)* This system was designed to evaluate the response characteristics of photodetectors operating at wavelengths in the 1 micron and 8-12 micron range. A Quartz-Tungsten-Halogen source was used for visible and near-IR energy, and a dedicated IR element provided gray-body radiation with a peak at 1150 Kelvin. A monochromator was employed in conjunction with a six-position filter wheel to provide precise control of energy incident on the photodetectors. Variations in the efficiency of components were compensated for through normalization based on the energy incident on the photodetectors. An intuitive, computer-based interface was developed to automate data collection, and provided numeric and graphic representations of data as it is being collected. At completion, data is exported to a spreadsheet file. A commercial silicon detector was successfully characterized, and accurate voltage response and responsivity curves were generated. A pyroelectric detector was used to verify proper operation of gratings and filters at infrared wavelengths. The system is suitable for its intended purpose, and will be capable of characterizing detectors designed to operate in the 3-5 micron range with the installation of appropriate filters and gratings.			
14. SUBJECT TERMS Detector, Photodetector, QWIP, Responsivity, Monochromator, Characterization, Characteristic Response, Detectivity, LabVIEW, Virtual Instrument, Optics, Photonics			**15. NUMBER OF PAGES** 85
			16. PRICE CODE
17. SECURITY CLASSIFICATION OF REPORT Unclassified	**18. SECURITY CLASSIFICATION OF THIS PAGE** Unclassified	**19. SECURITY CLASSIFICATION OF ABSTRACT** Unclassified	**20. LIMITATION OF ABSTRACT** UL

THIS PAGE INTENTIONALLY LEFT BLANK

**COMPUTER-CONTROLLED PHOTODETECTOR CHARACTERIZATION
SYSTEM (DESIGN AND CONSTRUCTION)**

Bryan E. Herdlick
Lieutenant Commander, United States Navy
B.S.E.E., University of Dayton, 1986

Submitted in partial fulfillment of the
requirements for the degree of

MASTER OF SCIENCE IN APPLIED PHYSICS

from the

**NAVAL POSTGRADUATE SCHOOL
December 2002**

Author: Bryan E. Herdlick

Approved by: Gamani Karunasiri
                  Thesis Advisor

                  Scott Davis
                  Second Reader/Co-Advisor

                  William R. Maier II
                  Chairman, Department of Physics

iii

THIS PAGE INTENTIONALLY LEFT BLANK

ABSTRACT

This system was designed to evaluate the response characteristics of photodetectors operating at wavelengths in the 1 micron and 8-12 micron range. A Quartz-Tungsten-Halogen source was used for visible and near-IR energy, and a dedicated IR element provided gray-body radiation with a peak at 1150 Kelvin. A monochromator was employed in conjunction with a six-position filter wheel to provide precise control of energy incident on the photodetectors. Variations in the efficiency of components were compensated for through normalization based on the energy incident on the photodetectors. An intuitive, computer-based interface was developed to automate data collection, and provided numeric and graphic representations of data as it is being collected. At completion, data is exported to a spreadsheet file. A commercial silicon detector was successfully characterized, and accurate voltage response and responsivity curves were generated. A pyroelectric detector was used to verify proper operation of gratings and filters at infrared wavelengths. The system is suitable for its intended purpose, and will be capable of characterizing detectors designed to operate in the 3-5 micron range with the installation of appropriate filters and gratings.

THIS PAGE INTENTIONALLY LEFT BLANK

TABLE OF CONTENTS

LIST OF FIGURES

LIST OF TABLES

ACKNOWLEDGMENTS

THIS PAGE INTENTIONALLY LEFT BLANK

I. INTRODUCTION

A. BACKGROUND

The purpose of this thesis was to design and construct a system that would be capable of accurately characterizing photodetectors designed to operate simultaneously at wavelengths in the 1 micron and 8-12 micron range. Conducted in parallel with thesis efforts focused on the design of such photodetectors, this system will be used to verify device performance and validate design algorithms. Additionally, it will support academic demonstrations and follow-on research and development. It was undertaken with intent to allow the Naval Postgraduate School to research and develop photodetectors for unique military applications.

As of the writing of this thesis, most infrared imaging systems and laser designation / tracking systems in use by the United States military depend on detectors that are designed to respond to energy from a very narrow part of the spectrum. Infrared detectors typically make use of atmospheric band-pass "windows" in the 3-5 or 8-12 micron regions, while laser designators and associated detectors operate in windows near 1 micron. Until recently, weapon systems were detector-limited and usually restricted to operating in only one of these windows. So-called "dual color" systems have been designed using two detectors to provide response in both the IR and UV ranges. Such an approach, when applied to heat-seeking missiles, is often employed to support improved tracking through flare rejection (e.g. SA-16 Gimlet) [Ref. 1]. Such a simple approach does not translate easily into more complex imaging systems such as Forward Looking Infrared (FLIR) and the Laser Spot Tracker (LST) or systems incorporating focal plane arrays. The F/A-18 Hornet, for example, carries a Nitehawk FLIR pod for infrared detection and tracking of targets (and also incorporates a laser designation system). However, the F/A-18 must carry a separate LST pod to identify targets being illuminated by laser designators on other platforms. The need for a separate pod to provide the operator a LST capability precludes use of a much needed weapon station. Such a multi-pod design also requires significant maintenance efforts to ensure that the LST is in proper alignment with other systems (e.g. "boresighting" with the FLIR, Heads-Up Display (HUD) and the air-to-ground radar). Additionally, it relies on accurate computer

integration of multiple source imagery to provide the operator with an image in the cockpit that accurately merges laser designation symbology with the target scene provided by the FLIR or ground-mapping radar.

The advent of quantum well photodetectors [Ref. 2 and Ref. 5 pp. 454-471] now presents an opportunity to reduce the level of complexity inherent in current systems. A single detector, tailored to operate in two or more of the aforementioned atmospheric windows simultaneously, could potentially remove both the hardware and software design challenges associated with integration of imagery from multiple sources. In the case of the F/A-18 it could potentially recover a valuable weapon station. In the case of the F-15, F-14 and F-16, an LST capability could be added to their present targeting system (e.g. the LANTIRN pod; Low Altitude Navigation and Targeting, Infrared for Night).

Designing and producing quantum well devices is a complex process that relies heavily on cutting-edge semiconductor growth techniques (e.g. molecular beam epitaxy [Ref. 3, p 7-43 and Ref. 4, p 569]). Due to the intricacy of their design, it is important to probe the response characteristics of these devices to validate the design algorithms. Such an evaluation requires repeatable, operational testing of each photodetector under controlled conditions. It is with this goal in mind that the computer-controlled photodetector characterization system (PCS) described herein was designed and constructed. The performance metric of choice is responsivity. Responsivity is a term that represents, for a given wavelength, the current flowing through the device (or voltage across the device) as a function of the optical power incident on the device [Ref 4, p. 650]. An example of the product to be generated by this system is depicted in Figure 1, below.
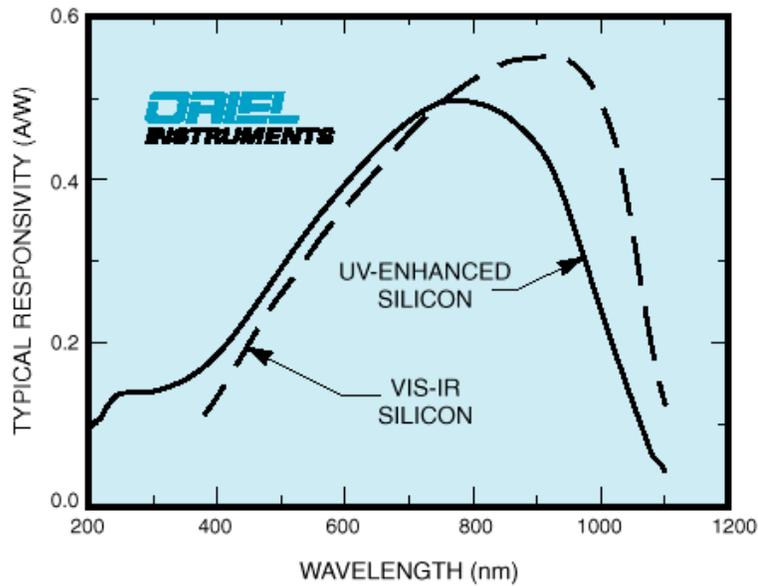
Figure 1.   Sample Response Curve (Silicon).
From: http://www.oriel.com/down/pdf/06071.pdf , 18:27 GMT, 2 December 2002.

B.   STRUCTURE OF THIS THESIS

A full appreciation for the characteristics of each component in the photodetector characterization system and the thought process behind their selection and modification are fundamental to informed, productive, safe use of the system. Therefore, in an effort to provide future users of this system with a single-source reference document for operation and follow-on development, this thesis is organized around the major components, the supporting optical hardware, and the controlling software. After a brief system overview that defines the four major modules of the system, each major component will be addressed with attention to design considerations and system optimization. Principles of optics, semiconductor electronics and system integration will be addressed as a matter of course since the identification and resolution of design challenges required a thorough understanding of the applicable principles from each of these fields. In the interest of readability, the bulk of specification sheets, operating checklists, data charts and other supporting material have been relegated to appendices. Unless otherwise stated, all part numbers provided are from the 2001 Oriel Instruments

3

catalog [Ref. 7]. A detailed parts list is included in Appendix I. While references are provided for all equations and more complex concepts, it is assumed that the reader possesses an undergraduate-level grasp of physics (particularly optics) as well as a fundamental understanding of basic electrical and systems engineering concepts.

C.   SYSTEM OVERVIEW

The system description will be addressed as an arrangement of four primary modules. Images of each of the modules are provided, and a basic schematic diagram of the system concludes this discussion. The first module was responsible for providing energy of narrow bandwidth, known wavelength and high spectral purity (the first independent variable in the evaluation). Components of the first module included a twin-lamp source, a filter wheel assembly, a monochromator equipped with three diffraction gratings and micrometer driven apertures, and a chopper-wheel that modulated the output energy at a known, fixed frequency. All of these components were mounted on a base-plate that ensured optimum alignment and supported easy adjustment of the optical height of the module. The first module is depicted in Figure 2.
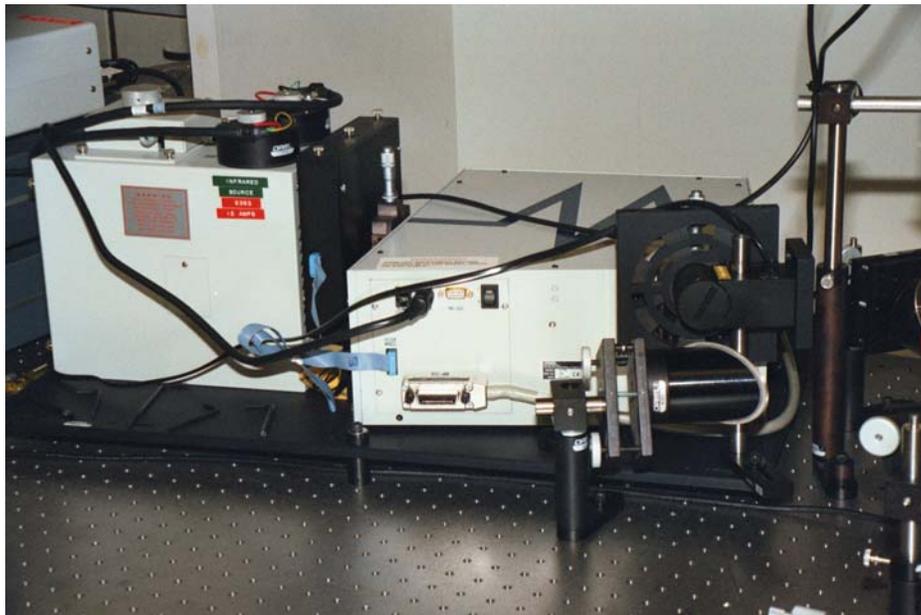
Figure 2.   Module One.

The second module was responsible for directing the energy to the detectors. Once the energy left the monochromator and was modulated by the chopper, it was routed to a beam splitter by a paraboloidal reference mirror that collimated the beam. The beam splitter then reflected equal amounts of energy to each of the detectors via two more paraboloidal reference mirrors. Each of the mirrors was supported by adjustable mounting hardware that allowed the operator to make minor positional changes to achieve optimum focusing of the Monochromator exit-slit image on each detector. Modules one and two are depicted in Figure 3. Note the reference detector mounted vertically above one of the mirrors (approximately at photo center), the silicon detector on a simple mechanical mount (breadboard) and the sliding rail assembly for moving the closed-loop refrigeration unit (Appendix I, Item I) into position for evaluating cooled detectors (Figure 3, upper right).
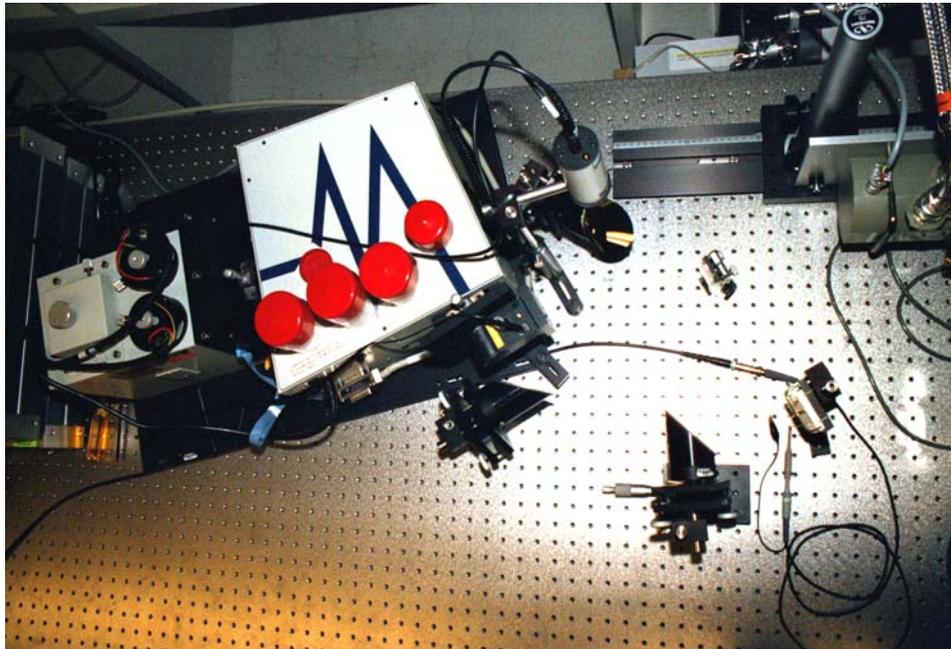
Figure 3.   Overhead Perspective of Modules One and Two.

The third module included a reference detector, the test article (also referred to in this document as the "detector under test", "test detector" or "sample") and their respective lock-in amplifiers. The reference detector was a pyroelectric device [Ref. 8, pp. 104-105] with a response curve that was designed to be essentially flat at wavelengths greater than 600 nm. Although the voltage measured at the reference detector was technically an independent variable, the flat response curve of the device permitted the data collection algorithm to generate the second independent variable (incident energy) which was then used in responsivity calculations. Voltage measured at the test detector was the dependent variable of interest.

The fourth module was comprised of the computer, its software and communication cables. Software developed specifically for this application was designed to provide a single operator control panel for execution of all aspects of photoconductor characterization testing. Real-time graphic displays of responsivity and detector voltages were design goals, as well as transfer of data to an output file in a format compatible with most spreadsheet software.
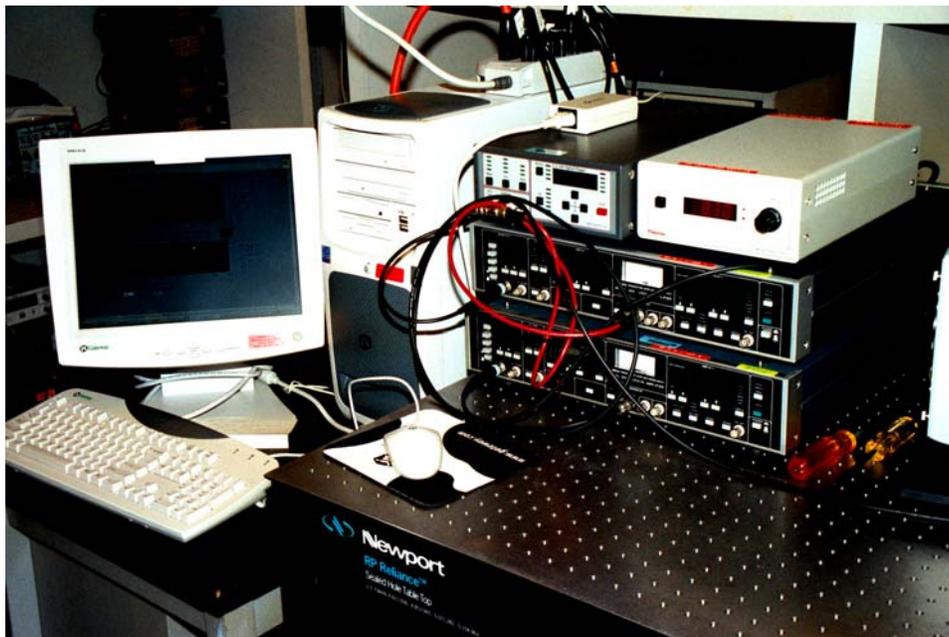
Figure 4.   Computer and Lock-In Amplifiers.

An image of the full system diagram is included here as Figure 5, with a corresponding schematic diagram (Figure 6) appearing on the following page.
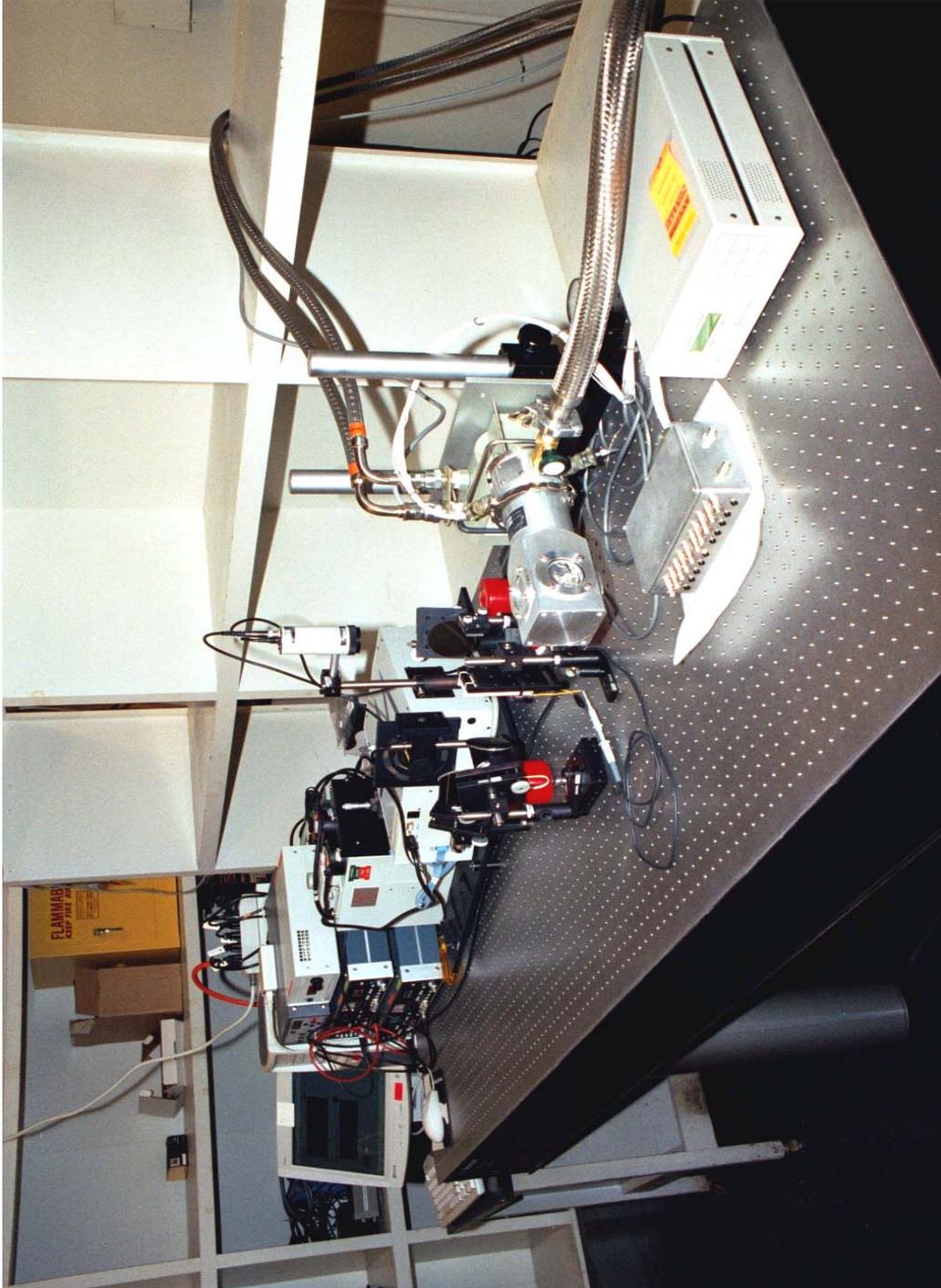
Figure 5.   The Photodetector Characterization System.

RS-232

GPIB

Lock-In Amplifiers

GPIB

sync

Chopper Controller

IR & QTH LAMPS

MONOCHROMATOR

Filter Control Signal

CHOPPER

REFERENCE DETECTOR

BEAM SPLITTER

DETECTOR UNDER TEST

Paraboloidal Mirror

Light / Energy

Electrical Connection

Communicaton Bus
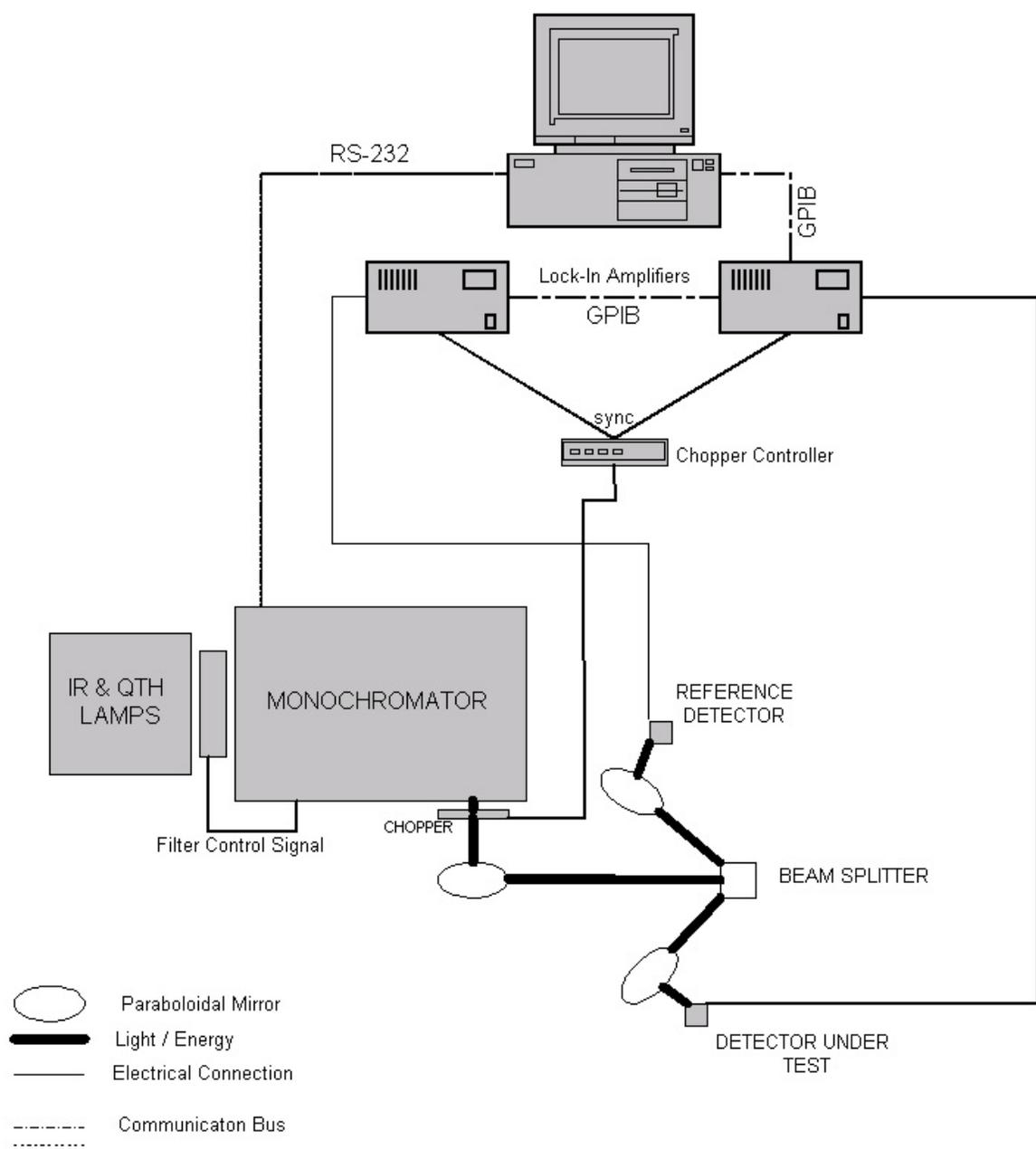
Figure 6.   Schematic Diagram (Full System).

II.   DESIGN AND CONSTRUCTION

A.   GENERAL

In order to characterize photodetectors operating in the 1 μm and 8-12 μm portions of the spectrum, components were selected to ensure optimum performance in those regions. Although outside the scope of the initial design effort, modification of the system was also undertaken to support broad-spectrum coverage for future applications. Design challenges were manifold. Many of the components that were selected, while meeting specific design requirements very well, often introduced additional deficiencies to the system that required compensation. A review of these design challenges follows, and provides the most effective insight into the system and its operation. Detailed performance specifications and a complete parts list for the system are provided in Appendix I.

B.   MODULE ONE: GENERATION AND CONTROL OF ENERGY

1.   Energy Source(s)

In an effort to meet the design requirement for evaluation of devices at approximately 1 μm and in the 8-12 μm band, while also providing flexibility for operation into the visible spectrum, two energy sources were required. The Oriel Instruments IR Element (Part No. 6363) was chosen for its almost constant emissivity (e.g. graybody radiation) in the region from 1 to 25 μm.

To provide energy at wavelengths associated with military laser designators (approximately 1 μm) and also to cover the visible spectrum (approximately 400-700 nm), a Quartz-Tungsten-Halogen (QTH) lamp was selected. The Oriel 6333 100W QTH lamp was designed to produce irradiance in excess of 10 milliwatts per square meter (at a distance of 0.5 meters) at wavelengths from 400 nanometers to 1800 nm [Ref. 7].

A universal monochromator illuminator was chosen to house the two elements. The illuminator included a cooling fan and a pivoting mirror that allowed the operator to select between the two sources. Each element was installed in a mounting base that permitted mechanical adjustment of the position of each element (to optimize alignment with respect to the mirror, ensuring illumination of the monochromator input aperture) and also provided for electrical connection to the power supply. The mounting base additionally ensured that the elements were aligned with the monochromator entrance slit (i.e. vertical to the optical table for this system).

A power supply with both voltage and current displays was selected to enable the operator to control the IR element according to the device specifications detailed in Table 1 (below) and to meet operating requirements for the QTH lamp to support the designed performance parameters described above (see also Figure 7, next page).

Table 1.   Operating Specifications (Oriel #6363 IR Element).

Voltage (Volts)	Current (Amps)	Power (Watts)	Surface Temperature (Kelvin)
13.0	12.8	166	1190
12.0	12.3	148	1160
11.0	11.7	129	1120
10.0	11.0	110	1075
9.5	10.6	101	1050
9.0	10.2	92	1030

From: Device specification sheet. See Appendix I for full document.

While achieving such broad-spectrum coverage from just two sources seemed a triumph in efficiency, two design challenges arose from the above component selections. First, the QTH lamp provided energy at all wavelengths within its operating spectrum simultaneously. Combined with the diffraction gratings in the monochromator, this presented a spectral purity issue that will be addressed later (e.g. higher order contributions from diffraction gratings). Additionally, incident energy could not be

considered a constant during an evaluation of a visual-NIR detector since, according to its design specifications, the irradiance of the QTH lamp varied across its operating spectrum. This (and other issues, identified separately) drove a requirement for normalization of data with respect to incident energy levels. This was ultimately accomplished with a reference detector (a detector of known spectral response). This concept will be fully developed in the discussions on the reference detector and application-specific software.
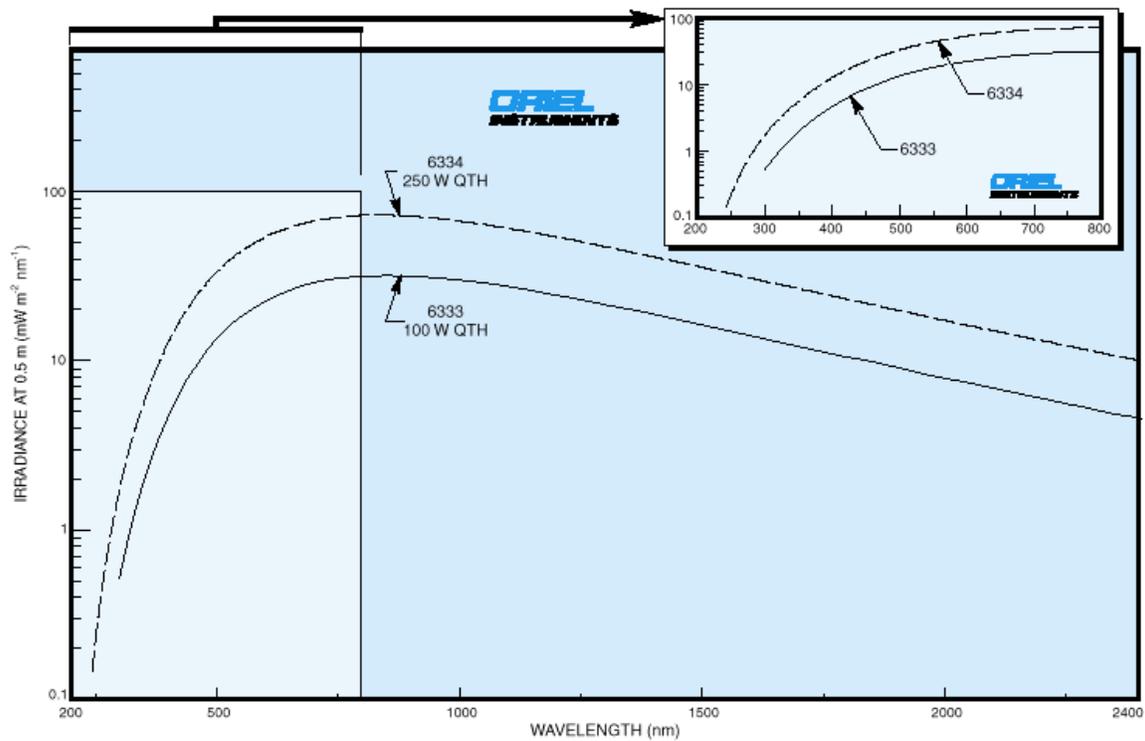
Figure 7. Performance Characteristics of the Oriel #6333 QTH Lamp.
From: http://www.oriel.com/down/pdf/calculation.pdf, (Fig 12), 00:20 GMT, 3 December 2002.

2. Monochromator

Monochromatic light for evaluation of optical systems and components has, historically, been obtained from the radiation of elements such as cadmium, mercury, hydrogen, helium and sodium [Ref 5, pp. 181-184]. While excellent for calibration purposes, the number of individual sources necessary to cover the broad spectrum required for this application would have been operationally inefficient and quite expensive. Since incrementally "sweeping" through a given spectrum on a controlled schedule was the cornerstone to generating the data, another means of generating monochromatic light was necessary. A monochromator (essentially a device to produce "single colors", as the name implies) typically uses multiple diffraction gratings, adjustable apertures and a computerized look-up table to achieve precise control of a near single-frequency output throughout a broad spectrum. The Cornerstone 260 monochromator, from Oriel Instruments, was chosen for its three-grating design. Meeting the design requirements for this application required great attention to the characteristics of the diffraction gratings, the size of the monochromator input and output apertures, and to the spectral content of the incident light.

Diffraction gratings [Ref 6, pp. 123-125] were the key component of the monochromator as they were responsible for the dispersion of light. Once spatial separation of incident energy into different wavelengths was achieved by the diffraction grating, the monochromator was designed to sweep the resulting beam across an exit slit that permitted energy of narrow bandwidth (a function of slit width) to exit the monochromator.
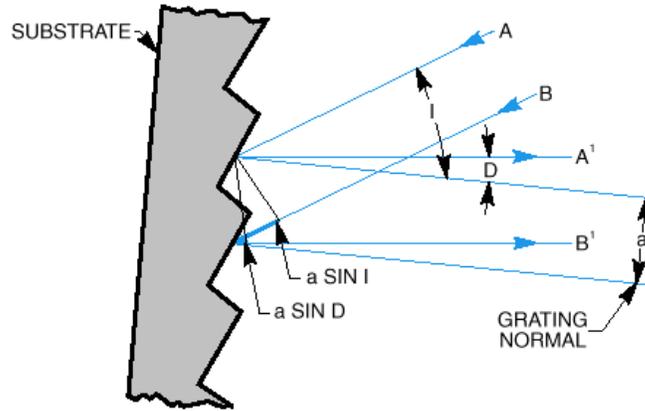
Figure 8.   Diffraction Grating Geometry.
From: http://www.oriel.com/down/pdf/04002.pdf, (Fig 1), 00:22 GMT, 3
December 2002.

Given the geometry depicted above, the grating equation takes on the following form:

$$a(\sin I + \sin D) = m\lambda \tag{1}$$

Variables are defined as: a = the distance between rulings on the grating; I = angle of incidence, measured from the grating normal; D = angle of diffracted light, measured from the grating normal; m = the order of the diffraction (an integer) and λ = wavelength.   Of interest, the angle D, if opposite the normal from the incident ray, assumes an opposite sign.

A different form of the grating equation was found to be more suitable for use the monochromator application adopted for this system. By defining an angle (θ) as the angle of the grating with respect to the zero-order position and another angle (ϕ) as half the angle between the incident and diffracted rays, the basic grating equation can be altered as follows:

$$m\lambda = 2a \cos\phi \sin\theta \tag{2}$$

where: $\begin{aligned} I &= \theta + \phi \\ D &= \theta - \phi \end{aligned}$

13

This form of the equation more clearly shows the effect of driving θ to zero. In such a case, the value of *m* becomes zero, and *all* wavelengths are reflected by the diffraction grating. When zero was selected for the monochromator wavelength, this forced the *m*=0 case and provided full spectral throughput from the monochromator (e.g. "white light", when the QTH lamp was selected as the source). This mode of operation proved extremely useful for visual alignment of components, since the image on the detectors was at maximum intensity and therefore easily visible to the operator [Ref. 7, Tutorial: Diffraction Grating Physics].

The monochromator alone cannot achieve the desired spectral purity when broad-spectrum energy is incident on a diffraction grating. Specifically, with multiple wavelengths incident on the grating, any number of wavelengths may be diffracted at a given angle. This is best understood as a matter of integer multiples, or "orders" of diffraction (i.e. *m*=1, 2, 3, 4… in the grating equation, above). For example, if a grating is being used to generate energy with a wavelength of 1000 nm from a broad-spectrum source (e.g. the aforementioned QTH lamp), the desired first order diffraction at 1000 nm will also include 2nd order diffraction components from 500 nm light incident on the grating as well as 3rd order diffraction components from 333.3 nm energy, etc. This effect is depicted in Figure 9, below. Since the grating itself cannot respond to the incident energy in any other way, the best approach to improving the spectral purity of the diffracted energy is to restrict the bandwidth of the incident energy (specifically: block the shorter wavelengths that are the source of the problem). Placing a long wavelength filter between the lamp and the monochromator was adopted as the best solution and is discussed in detail later.
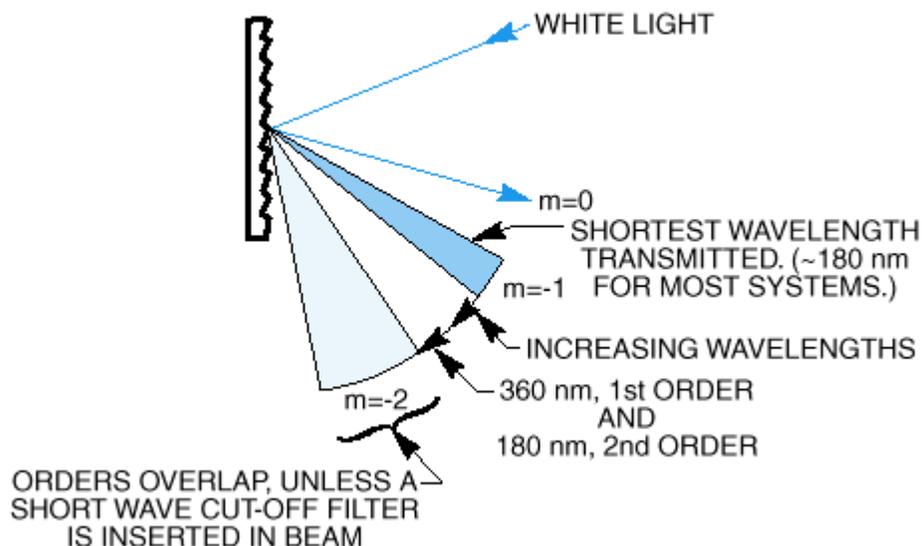
Figure 9.   Diffraction Grating (Overlapping Orders).
From: http://www.oriel.com/down/pdf/04002.pdf, (Fig 3), 00:22, 3 December
2002.

Up to three diffraction gratings could be installed in the Oriel CS-260 monochromator. Those chosen for this application are reflected in Table 2, below. Driven by the application presented in the introduction, regions of interest were initially identified as the 8-12 μm band common to Forward Looking Infrared (FLIR) systems and the 1 μm wavelength region common to U.S. and NATO military laser designators. Visible spectrum capabilities were incorporated to support system development, verification and validation using inexpensive detectors that were designed to operate at room temperature. Desired growth capability for the system included evaluation of detectors designed to operate in the 3-5 micron range, therefore the appropriate grating was purchased and is also included in Table 2.

Table 2.   Performance Specifications, Diffraction Gratings.

Oriel Part No.	Ruling Density (lines / mm)	Blaze Wavelength* (nm)	Efficiency (peak)	Operating Region (>20% efficient)
74066	600	400	80%	250-1300 nm
74067	600	1000	75%	600-2500 nm
74080**	150	4000	80%	2.5-9.6 μm
74082	75	7000	80%	4.5-19.2 μm

* Wavelength at which maximum efficiency is achieved (a grating design parameter).

** Procured for follow-on development only; not installed during system development.

A critical review of the diffraction grating performance specifications identified another contributor to variations in the intensity of the monochromator output. Peak efficiency is not a constant from grating to grating, and values as low as 20% are still considered to be within the operating region. This was yet another convincing argument for normalization of data with respect to energy incident on the detector (i.e. use of a reference detector).

3.   Filters and Filter Wheel

As mentioned earlier, addressing the high-order contributions from the diffraction gratings was accomplished by filtering the energy incident on them. Filters were selected based on the wavelengths of interest for this application. Cutoff wavelengths of 400 nm, 1000 nm and 8000 nm were initially selected, with additional filters at 2.5 and 5.25 μm selected to satisfy broad-spectrum capability for the system. The absorption of energy with wavelengths smaller than those of interest precluded generation of unwanted high-order contributions and improved the spectral purity of the monochromator output.

Table 3.   Long-Wavelength Filters and Filter Wheel Schedule.

Filter Wheel Position (1-6)	Oriel Part No.	Cutoff Wavelength (schedule)	Transmission	Intended Use
1	*TBD**	*TBD*	*TBD*	*TBD*
2	57353	600nm (620-1030 nm)	>85% (620 nm →)	Visual
3	57369	1000 nm (1030-2060 nm)	>85% (1030 nm →)	NIR
4	*TBD**	*TBD*	*TBD*	*TBD*
5	57955	8000 nm (8183 nm-∞)	~85% (8183-16639 nm)	8-12 micron IR
6	57345	400 nm (410-620 nm)	>80% (410 nm →)	Visual

* Note: The 5.25 μm filter (Oriel Part No. 57940) and the 2.5 μm filter (Part No.57925) were not installed during system development.

A computer-controlled six-position filter wheel was incorporated to rotate the correct filter into position based on a user-defined look-up table, and the wavelength commanded by the software. To avoid the aforementioned high-order contributions, the filter schedule employed each filter from its cutoff wavelength to a value twice that of cutoff (i.e. where the second order of the cutoff wavelength is reached and higher order contributions would again become problematic).   This guideline was key in both selecting the filters and generating the user-defined look-up table for control of the filter wheel. Table 3, above, details the filters and schedule employed for this system.   The apparently random ordering of filters in the wheel was a result of mechanical compatibility between filters, filter holders and mounting clearances in the filter wheel and housing.

4. Entrance and Exit Apertures

The entrance and exit slits of the monochromator also have an impact on the spectral purity of the energy provided by this module of the system. Since the diffraction grating spatially separates the wavelengths, allowing them to pass through a slit wider than necessary broadens the bandwidth of the monochromator. Put simply, beyond a given size, greater slit width = reduced resolving power = greater bandpass = reduced spectral purity. Specifically, this may be represented as

$$\triangle \theta = n \triangle \lambda / h \cos \theta \qquad (3)$$

where $\triangle \theta$ is the angular separation between two spectral lines that differ by $\triangle \lambda$, h is the separation of slits in a conventional diffraction grating, and n is the diffraction order being considered [Ref 6, pp. 123-125]. Thus, the width of the monochromator exit slit, at a given distance from the grating, is analogous to $\triangle \theta$. Therefore (to reiterate), for any given diffraction order, some bandwidth $\triangle \lambda$ will be passed depending on slit width.

As with all design considerations, there are compromises. In this case, as the slit width is reduced, the energy throughput for the monochromator is reduced. For example, in the case of an entrance slit that is fully illuminated by a uniform broadband source, doubling the slit width (assumes input and exit slits are of equal size) results in a factor-of-four increase in energy throughput. For non-uniform sources (such as the QTH lamp in this system) and slit widths greater than the source image size, the increase corresponding to doubling the slit width is somewhere between a factor of two and four [Ref. 9] The preceding example made it apparent that adjustability of the entrance and exit apertures would be critical to optimizing monochromator performance, therefore, micrometer driven slit assemblies were installed. (Computer controlled assemblies were considered, but rejected due to expense).

An evaluation was conducted during system construction. By operating the monochromator at visual wavelengths and adjusting the width of the slits (individually and in conjunction) the effects described earlier became immediately apparent. Specifically, varying intensity and changes in the spectral purity of the energy were

evident in the slit image projected on a piece of white paper inserted just in front of the detector.

Given entrance and exit slits of equal width, and the specifications for the gratings selected for this system, the bandpass characteristics reflected in Table 4 may be easily calculated from reciprocal dispersion (nanometers of bandpass per millimeter of slit width) which is a grating performance specification provided by the manufacturer. The competing guidelines for slit width selection, the experience gained from the qualitative evaluation described above and the expected size of the detectors suggested a nominal slit width of 1mm to simplify incident energy calculations (discussed later).

Table 4.   Bandpass of Gratings (aperture width = 1mm).

Grating Position (Part Number)	Reciprocal Dispersion (nm/mm)	Bandpass (Blaze Wavelength)
1 (74066)	6.5	**6.5 nm** (400 nm)
2 (74067)	6.4	**6.4 nm** (1000 nm)
3 (74082)	51.7	**51.7 nm** (7000 nm)
Alternate Grating (74080)	25.8	**25.8 nm** (4000 nm)

C.   MODULE TWO: BEAM CONTROL (OPTICS)
1.   Beam Splitter

A coarse-grating beam splitter was employed to direct half of the monochromator output to the device under test and the other half to a reference detector (for subsequent computation of incident energy intensity and normalization of data). Coated with Aluminum Silicon Monoxide (AlSiO), the Oriel model 38111 was designed to exhibit a reflective efficiency of greater than 80% for most of the spectrum above approximately 370 nm, and an efficiency of greater than 90% for wavelengths greater than about 1.3 μm

[Ref 7; Oriel device data for AlSiO reflectance vs. wavelength].   The reflected beams exit at an angle of 60 degrees from the grating normal and are of equal intensity, regardless of variations in reflectance. Figure 10, below, depicts a notional coarse-grating beam splitter. Conveniently, the compensation for variations introduced by other components (e.g. the diffraction gratings in the monochromator and filters in the filter wheel) is also effective in addressing deviations in beam splitter reflectance. Again, techniques and components involved in data normalization will be discussed later.
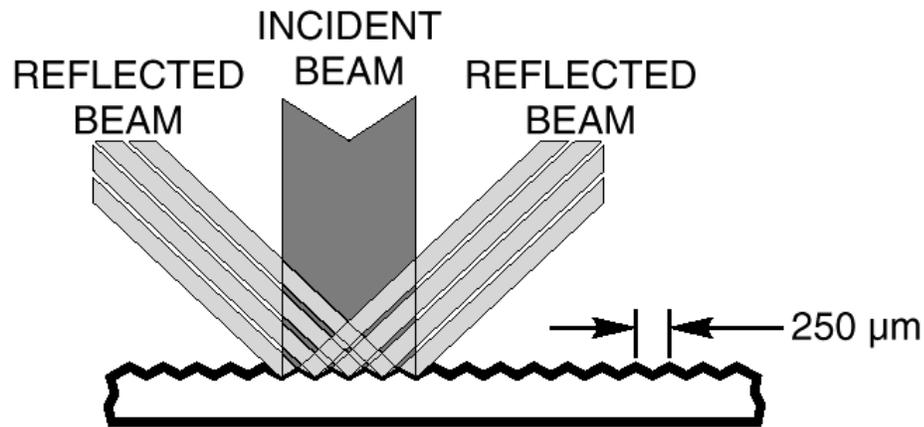
Figure 10.   Coarse-Grating Beam Splitter (General).
From: http://www.oriel.com/netcat/VolumeIII/Descrippage/v3t5cgbs.htm,
Schematic Drawing, 01:35 GMT, 3 December 2002.

2.   Paraboloidal Reference Mirrors

The use of a plane grating (e.g. the beam splitter) requires collimating and focusing through the use of mirrors or lenses [Ref 6, p.125]. Specifically, directing the energy between components without altering the image of the monochromator exit slit was necessary to ensure that the incident energy at each detector was effectively the same.   Infrared absorption concerns precluded the use of low-cost solutions such as lenses or back-coated mirrors. Therefore metal, paraboloidal mirrors (Figure 11) were

used to achieve focusing, collimating and directional control of the beam. The mirrors selected were characterized by a perpendicular focal distance ("V" in Figure 11) of 4.7 inches, which supported adequate separation of components on the optical table. The size of each mirror's reflective surface exceeded the extent of the monochromator exit slit image. With the exit slit of the monochromator placed at the focus of the paraboloidal mirror, parallel ray alignment within the beam (collimation; no dispersion) was ensured along the longitudinal axis of each mirror (perpendicular to its base). Similarly, the collimated beam, once diffracted by the beam splitter, was focused on each of the detectors by identical paraboloidal mirrors, yielding unity magnification. Mounting each mirror on adjustable mounting hardware, which included a "moveable hole", an adjustable optical rod, and a "tilt-table", made provisions for minor adjustments to beam direction. See Appendix I for part numbers and specifics.
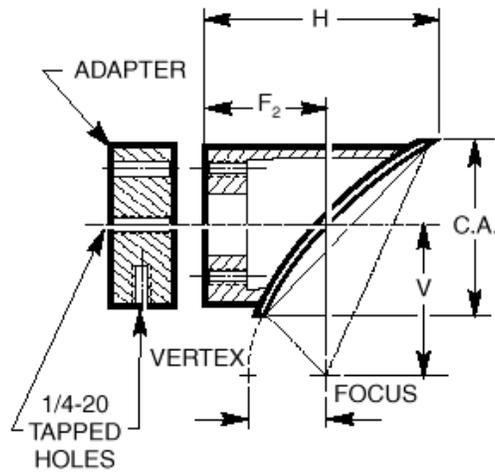
C.A.	H	V	F_2	Oriel Part No.
2.5 inches	2.92 inches	4.7 inches	1.5 inches	45347

Figure 11.   Paraboloidal Reference Mirror.

From: http://www.oriel.com/netcat/VolumeIII/Descrippage/v3t4para.htm, Schematic

Drawings, 01:38 GMT, 3 December 2002.

D.   MODULE THREE: DETECTION AND MEASUREMENT

1.   Lock-In Amplifiers

Lock-in amplifiers were incorporated into the system for their ability to significantly improve the signal-to-noise ratio. A lock-in amplifier is designed to rely on A/C techniques (signal processing) to measure DC or slowly varying signals. In order to employ a lock-in amplifier, the signal to be measured must be modulated at a known, fixed frequency while noise sources remain unmodulated. In this system, an optical chopper (Figure 12, below) was used to break the beam exiting the monochromator at a fixed frequency. The rotating disk was selected and positioned to alternately break and

pass the beam completely. Specifically, a disk with openings smaller than the largest dimension of the beam exiting the monochromator would not completely attenuate the beam and maximum amplitude would not be achieved in the AC signal produced. The chopper controller was set to a frequency that met the operating limitations of the reference detector (between 8 and 500 Hz, ideally) and yet avoided known noise sources such as the 60 Hz line voltage frequency, low frequencies where 1/f noise dominates, and harmonics of frequencies lower than the chopping frequency (e.g. 120, 180, 240 Hz, etc).
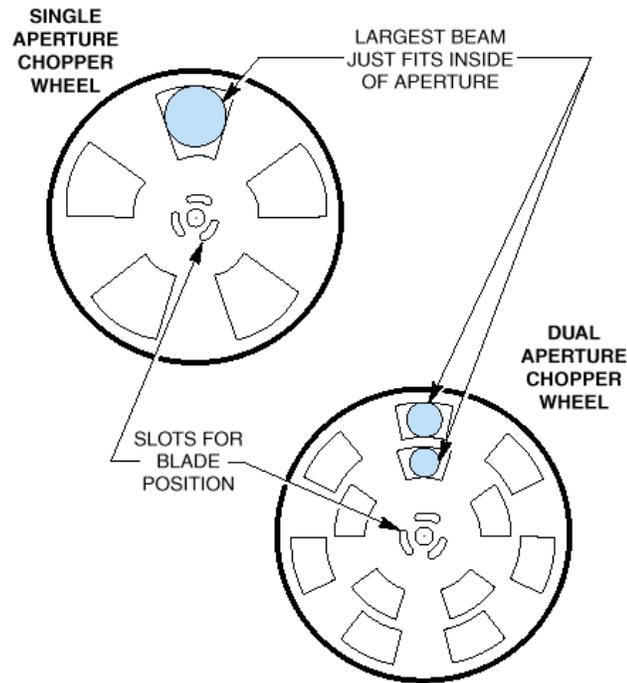
Figure 12. Optical Chopper.
From: http://www.oriel.com/down/pdf/06096 23:30 GMT on 1 December 2002

The lock-in amplifier, provided with a synchronizing pulse from the chopper controller, was designed to position an adjustable bandpass filter at the frequency associated with the signal to be measured. In doing so, noise outside this bandpass is rejected and the signal-to-noise ratio increases, supporting the measurement of signals that would otherwise vanish in the noise floor. For the Princeton Applied Research Model 5210 used in this system, bandpass is fixed at 1Hz about the synch frequency.

Author's Observation: The signal processing techniques employed by lock-in amplifiers is quite similar to methods used in many air-to-air missile seeker systems. By employing an approach of "selection-before-detection" (as it is described to weapon system operators during training), the amount of noise that the detection circuit is forced to process is significantly reduced. The key, as stated above, is providing the circuit with a pretty good idea of what it is looking for and where to find it. Another similarity in detection systems is the optical chopper that is almost identical to the early reticles used in the Sidewinder heat-seeking missile.

2. Reference Detector

Since the responsivity of a detector is commonly described in units of either volts-per-watt or amps-per-watt (depending on the mode in which the device is operated) vs. wavelength, these values must therefore be measured at each wavelength in order to accurately characterize the spectral response of the device. As previously noted, variations were inherent in the efficiency of optical components in the first module (e.g. QTH lamp, filters, and diffraction gratings) as well as in the beam splitter in the second module. Therefore, the incident energy at the detector could not be considered a constant at different wavelengths. Ultimately, the only way to verify the amount of energy incident on the test detector was to measure it.

Measuring the energy incident on the test detector was achieved by separating the beam equally with the aforementioned coarse-grating beam splitter and directing half of the energy from the monochromator onto a reference detector. The detector selected for this role was chosen for its essentially "flat" response over the wavelengths being considered (note: the visible spectrum was not considered a driver for component selection in this case). The Oriel 70124 pyroelectric detector-head was designed to provide a response of 1000 V/W with a cut-on wavelength of approximately 600 nm (see Figure 13, below), which is due primarily to the KRS 5 window on the device. As a pyroelectric device, a modulated signal was necessary to generate a signal [Ref. 8, pp. 104-105]. Conveniently, the optical chopper at the monochromator output satisfied this requirement in addition to making its contribution to the signal processing effort.

24
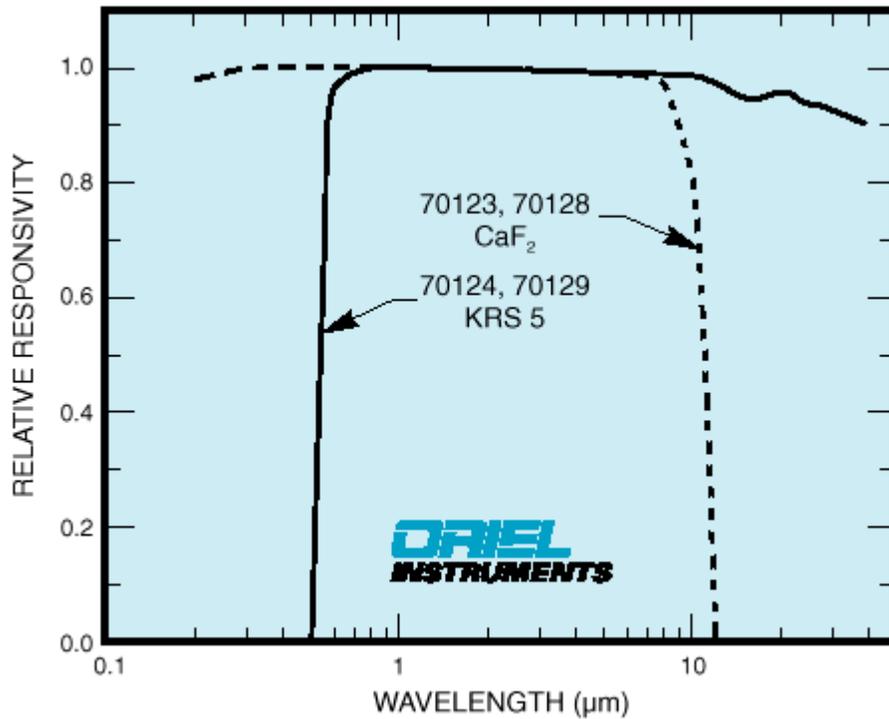
Figure 13.   Reference Detector Response Curve (Oriel #70124).
From: http://www.oriel.com/homepage/down/pdf/06029.pdf, (Fig 14), 01:58
GMT, 3 December 2002.

Given the response characteristics of the reference detector and its dimensions (5 mm diameter), the irradiance at any given wavelength (in W/mm^2) was then calculated from the equation on the next page. Longitudinal extent of the slit image far exceeded the 5 mm diameter of the detector, so the only alignment issue was to ensure that the slit image fell across the center of the detector. Techniques for achieving this are outlined in the operating guidelines at the end of this document.

$$E = (1W/1000V)(V_{ref})/(5mm^2) = (V_{ref})/(5000V \bullet mm^2/W) \qquad (4)$$

Where: Illuminated area = 5mm^2 (5mm diameter x 1mm wide slit image)

E = irradiance (W/mm^2)

V$_{ref}$ = voltage measured at the reference detector (volts)

In the above equation, the irradiance incident on the reference detector is calculated from the responsivity of the reference detector (1000V/W) and the voltage measured at the reference detector (Vref), yielding power in watts. Since incident energy has units of watts per area, the illuminated area of the reference detector (5 mm^2; 5 mm detector diameter, illuminated by a 1 mm wide slit image) must be used in the denominator. The resulting value has units of watts per millimeter squared, as desired, which was then used to normalize the voltage response of the detector under test. This was accomplished in the data collection and processing segments of the software and is discussed shortly.

E.   MODULE FOUR: COMPUTERIZED CONTROL OF THE SYSTEM
1.   Software and Device Interface

Since characterizing a detector required selection and control of both diffraction gratings and filters, time averaging of data, data collection, calculation of responsivity and exporting data to a spreadsheet, computer control and semi-automation was a foregone conclusion in the design of this system. The monochromator, lock-in amplifiers and chopper controller were all designed to support computer control via general-purpose interface bus (a.k.a. GPIB or IEEE-488) and/or the older RS-232 serial bus. The monochromator, in fact, *required* computer support (the baseline device was shipped with no stand-alone control panel). A language that could control such a diverse group of devices while simultaneously supporting software development for data collection, processing and system integration seemed an enormous task at first, but LabVIEW [Ref. 10] was an ideal solution. This language relied on a graphical user interface for programming and is a giant leap beyond the line-by-line approach of FORTRAN and

26

C++. The flow-charting skills common to punch-card programming were extremely useful in making the transition to LabVIEW since the language reduces programming to a process of graphically arranging functional blocks into case structures and logic-trees. The troubleshooting tools, help functions, tutorials and examples were found to be extremely helpful. That being said, the learning curve was found to be incredibly steep and proficiency (measured by successful creation of a working system) required more than two months of dedicated effort and a number of "technical assist visits" from the manufacturer.

While LabVIEW can be used to develop software for any number of purposes, the arena in which it sets itself apart is in application to electronic instrument simulation and control. In many cases LabVIEW can almost completely replace a piece of test equipment (e.g. oscilloscope, voltmeter, etc.) and these virtual instruments (VIs) are some of the better offerings in the examples and tutorials available in the full development suite. For more specialized equipment that may be controlled via GPIB or RS-232, subroutines known as sub-VIs are available as programming tools for passing command strings. At the next higher level of complexity, some newer instruments (and those older devices that have become industry standards) often come with LabVIEW VIs included in the supporting documentation and equipment. The monochromator and the lock-in amplifiers both fall into this category. These device-specific VIs were useful in performing operational checks of each piece of equipment and in developing an over-arching VI for the photodetector characterization system as well.

2.   **Software Development**

The initial driver in developing the PCS VI was meeting communication requirements for the monochromator and the lock-in amplifiers. Initially the GPIB was tasked with supporting all communications and only one GPIB card was installed in the controlling computer. During system integration and software development, a major conflict was identified in that the monochromator dominated the interface bus when a scan was being conducted. Unfortunately, this precluded collecting voltage values from the lock-in amplifiers! Luckily, the CS260 monochromator ships with both GPIB and

RS-232 compatible VIs, which made it a relatively simple evolution to transition to dual-bus operations. In the final arrangement, the RS-232 bus was dedicated entirely to monochromator communications and the GPIB was used only for the lock-in amplifiers,

The approach that was identified as most effective for software development was to work backwards from the end product (generating a responsivity curve from measured voltage values) and then to expand the software into a full-system VI. The first step involved creating a data collection and processing (DCP) VI. This VI was created as a limited scope effort. As a stand-alone simulation, no requirement for device communication or control was imposed. As previously mentioned, the primary variables in the process were identified as the wavelength being generated by the monochromator and the voltages measured at each of the two detectors. Simulations were created in the DCP VI for each of these variables. For each simulated wavelength, the software was designed to sample and average the two simulated voltage values in anticipation of slight variations in actual voltage levels. The next calculation performed by the data processing software was to generate values for the responsivity of the test detector. Since the beam splitter was designed to direct the same amount of energy to each detector, the irradiance measured at the reference detector was considered to be the same as that incident on the test detector. To generate responsivity values for the test detector at each wavelength, the voltage measured at the test article was divided by the total energy incident on the device. Specifically, the irradiance calculated from reference detector measurements was multiplied by the total area of the test detector that was illuminated by the slit image (units: mm^2). For the purposes of system development, alignment and operational checks, test devices were fully illuminated by the 1 mm wide slit image. The DCP VI also provided for graphic display of detector voltages and responsivity.

The final task of the DCP VI was to export all data to a file in a format compatible with spreadsheet software such as Microsoft Excel or Lotus 1-2-3. This was accomplished by incorporating a sub-VI available from the LabVIEW development suite. Development of the DCP VI provided on-the-job education and training that proved critical to exploration of the monochromator and lock-in amplifier VIs and, ultimately, to the successful development of an application-specific VI for the photodetector

28

characterization system. Additionally, the DCP VI will provide an outstanding tool for follow-on software development and as an educational tool for future operators of the PCS.

Rather than starting from scratch in developing a full-system VI for the photodetector characterization system, exploratory analysis of the VIs that were shipped with the monochromator and lock-in amplifiers presented an alternative. Since it was determined that the monochromator VI was running essentially full-time during a scan cycle, it was selected as the starting point for development of the full-scale PCS VI. Two major steps were required to transform the monochromator VI into an application specific VI. First, the data collection and processing algorithm had to be incorporated into the monochromator VI. Second, the simulation sequences imbedded in the DCP VI had to be replaced with "live" connections (i.e. to the sources of wavelength and detector voltage). In the case of wavelength, this was accomplished with a direct connection as the two VIs were merged. Accessing the voltage values during each execution of the sample-and-hold sequence was accomplished by calling the lock-in amplifier VI as a sub-VI and "polling" the instrument for the voltage value being measured.

Figure 14, on the next page, depicts the hierarchical assembly of the PCS VI. An understanding of this nested-loop and embedded-VI approach to programming is essential to understanding the flow of information within the PCS VI and to tailoring the software to specific applications (should such modification be desired in the future). Screen capture images of the PCS VI wiring diagram are provided in Appendix III.
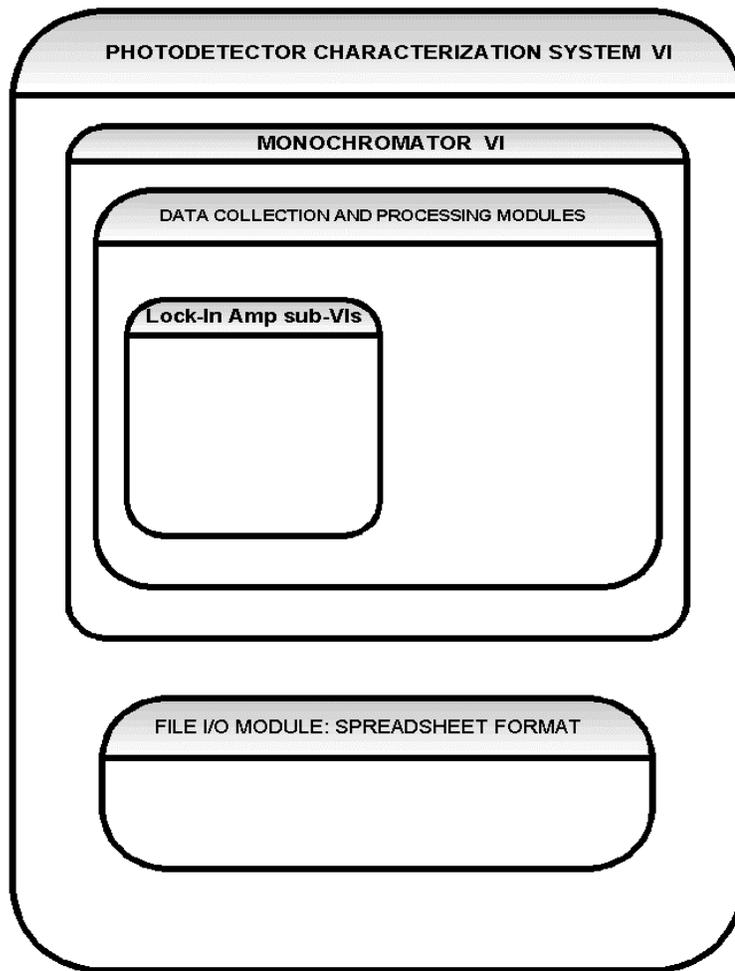
Figure 14.   Software Hierarchy (PCS; LabVIEW VI).

The front panel of the Photodetector Characterization System VI was designed to provide numerous real-time displays for operator monitoring of the evaluation process (Table 5 and Figure 15). Availability of this information was required to support multi-tasking within the laboratory (i.e. the operator should be made aware of the time required to complete the evaluation such that he/she may tend to other tasks). The display was also designed to support troubleshooting through real-time evaluation of the data (i.e. identification of unwanted perturbations or other unexpected results). When "go scan" is commanded, the data collection process is designed to begin and route the following information to the computer screen:

Table 5.   Primary Front Panel Displays for Conducting Evaluations.

VALUE	DISPLAY FORMAT	UNITS
Responsivity of Test Detector	Graphic	volts / watt vs. nanometers
Detector Voltages	Graphic	volts vs. nanometers
Detector Voltages	Numeric	MV
Time Remaining Current	Numeric	Minutes (estimate)
Wavelength	Numeric	nanometers
Samples Remaining	Numeric	Countdown from 10 to 0
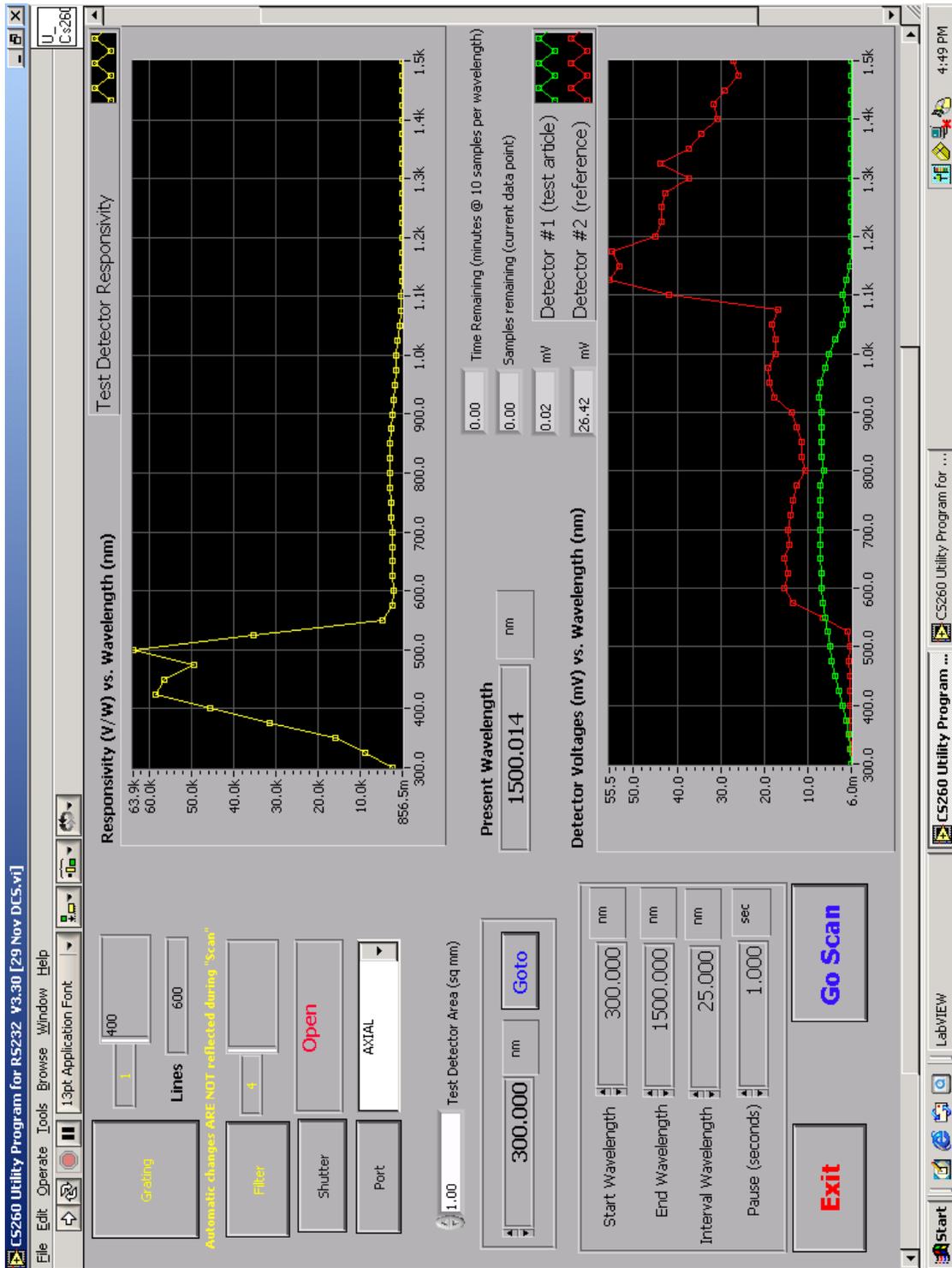
Figure 15.   PCS Front Panel (top graph: responsivity; bottom graph: voltage response)

Note the inflection points displayed in Figure 15 on the previous page. Specifically, the operating spectrum of the silicon detector is accurately depicted as beginning around 300 nm and ending at approximately 1150 nm (note the voltage response curve that never exceeds 10 mV), the cut-on of the reference detector at approximately 550 nm (note the voltage response curve that reaches almost 55 mV). Although the system was obviously not optimized for characterizing a silicon detector at the time this evaluation was conducted (i.e. the reference detector cannot be used to measure incident energy below 600 nm), the results were invaluable to the designer as a method of probing the performance of the system during design and calibration.

At the completion of a data collection event (scan), the system is designed to prompt the operator to enter a file location and file name for data storage. Data is then exported as a delimited text file that is compatible with most spreadsheet software. Microsoft Excel was used for follow-on data reduction and analysis.

THIS PAGE INTENTIONALLY LEFT BLANK

III.   MECHANICAL ALIGNMENT

In order to ensure maximum illumination of the monochromator input aperture, optimum positioning of the source elements had to be achieved. The long axis of the radiating element had to be aligned with the long axis of the input aperture, and the image of the source had to fill the input aperture. Specific guidelines for arranging components to ensure maximum monochromator throughput [Ref. 9] were met by mounting the monochromator and the illuminator on a base-plate designed for that purpose (see Figure 2).   In addition to optimizing the positioning of components, the base-plate also accommodated installation of the filter wheel (mounted between the illuminator and monochromator) and the optical chopper (at the output slit of the monochromator). Perhaps the greatest single advantage to using the base-plate was the ability to alter the optical height of the first module during developmental construction.

Specifically, near the end of the design and construction phase, a decision was made to mount the closed-cycle refrigeration head on a sliding track to allow it to be moved into position for evaluation of devices requiring cooling, or out of the way for evaluation of devices that could be mounted simply and operated at room temperature. This change elevated the optical height of the table (i.e. the plane formed by the beam of light / energy) by 1.5 inches and required repositioning of all components. The base plate maintained proper alignment of the aforementioned components and greatly simplified this process.

Mechanical alignment of components also included proper positioning of the beam splitter, mirrors and detectors to ensure proper illumination. In every case (subject to financial constraints) the greatest degree of adjustability was incorporated into the design.   Operating the monochromator with the wavelength set to zero provided a maximum-intensity, visible image to support initial alignment. In addition to manually directing the beam onto the detectors, course focusing was also accomplished. Once this had been achieved, the voltage levels displayed on the respective lock-in amplifiers were

referenced to further improve alignment. Ideally, this procedure should be completed prior to each data collection run with the equipment, and at least after detectors are changed or any of the components are repositioned.

IV. OPERATIONAL VERIFICATION

A. VISIBLE-SPECTRUM (USING A SILICON DETECTOR)

Although the system was not optimized for use with visible-spectrum detectors, the use of a silicon detector [Ref 8, p. 267] during system construction and alignment was convenient since silicon operates well at room temperature in the photovoltaic mode. Measurement of the voltage response of the silicon detector and reference detector provided a reasonable assurance that both devices and the characterization system were operating normally. Specifically, the voltage response curves were found to accurately reflect the expected spectral bandwidth of each device. Responsivity of the silicon detector could only be verified for that portion of the spectrum where both detectors were operational (e.g. approximately 600 to 1100 nm). A peak responsivity value was obtained at approximately 800 nm for the test detector, which compares well with the UV enhanced curve in Figure 16. Note that the comparison here is between shape, scale and location of the curves with respect to wavelength. For the responsivity of the notional device represented in Figure 16 to be converted from Amps per Watt to the units generated by the PCS (Volts per Watt), values for load and internal resistance would be required.
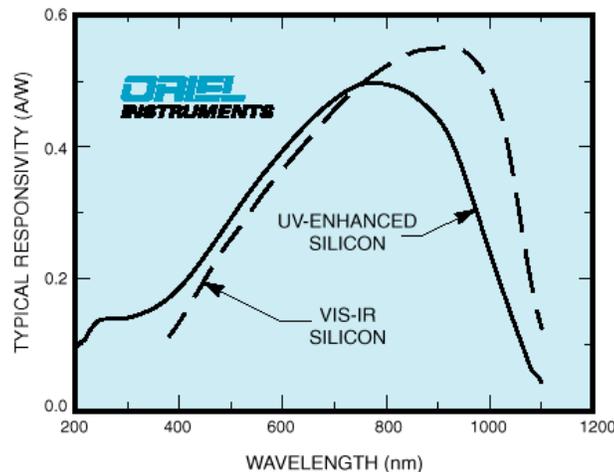
Figure 16.   Typical Responsivity of Silicon.
From: http://www.oriel.com/down/pdf/06071.pdf, 18:27 GMT, 2 December 2002.
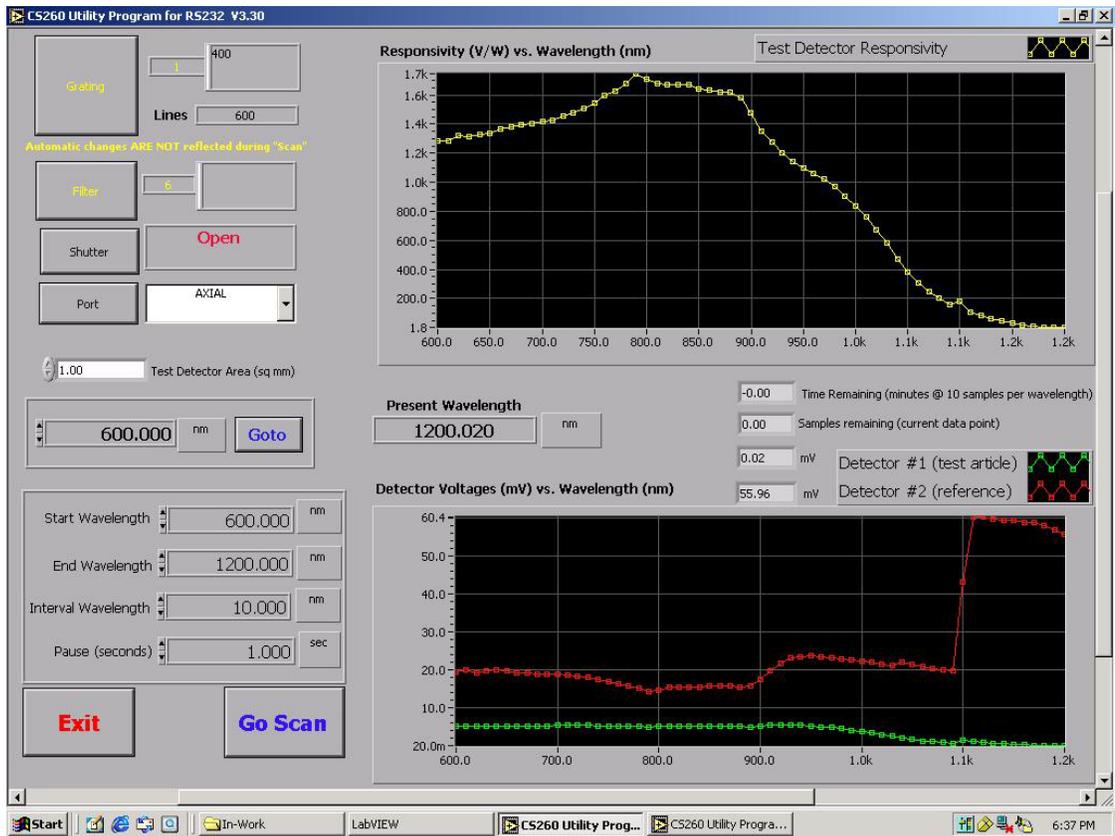
Figure 17.   Responsivity of Silicon (top graph)

Due to the scale of the graphs in Figure 17, deviations in the voltages measured at the detectors are not immediately apparent. In order to represent the full spectral bandwidth of the silicon device (~ 300 to 1200 nm) a separate scan was conducted with the goal of collecting only voltage values (remember, below 600 nm, responsivity calculations are erroneous due to the responsivity of the reference detector). When inspecting the curve generated from spreadsheet software (Figure 19; from Microsoft Excel, in this case), the voltage perturbations are clearly evident. The effect of normalization is immediately apparent in the comparatively smooth shape of the corresponding   responsivity   curve   (Figure   18).
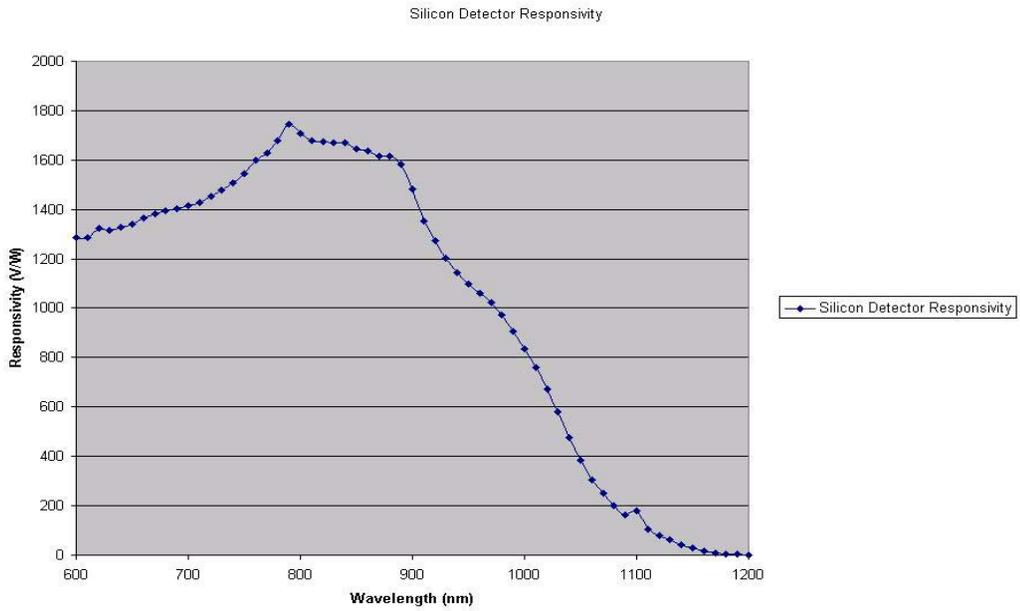
Figure 18.   Responsivity of Silicon (Spreadsheet Output).
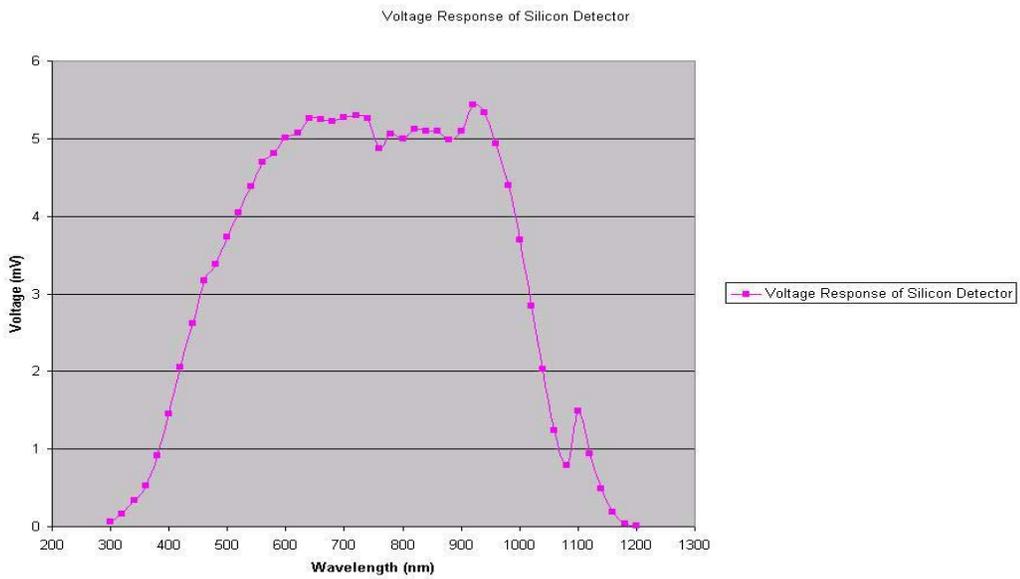
Figure 19.   Voltage Response of Silicon Detector.

B.   INFRARED REGION (USING THE REFERENCE DETECTOR)

To ensure that the system operate as intended in the IR region of the spectrum, the reference detector was used to probe the grating and filter performance with the source set to a temperature of approximataly 1150 Kelvin. A blackbody radiation curve for an 1150 Kelvin source is provided as Figure 20.   Figure 21 depicts the shift of the apparent maximum by the diffraction grating due to its blaze wavelength of 7 microns. Figure 22 further shows that the system effectively controls the energy exiting the monochromator by the insertion of a long-wave filter with a bandpass beginning slightly above 8 microns.

The Quantum Well Infrared Photodetector for which this system was originally designed had not completed fabrication at the time this thesis was written. No other 8-12 micron detectors were available to validate the PCS operation in the infrared. An attempt was made to assess system operation at infrared wavelengths using an Indium Antimonide detector (InSb; 3-5 micron operating range), but the device was damaged during its installation into a chip carrier. Unfortunately, no other infrared detectors were readily available for an evaluation similar to that conducted with the silicon device. While the system operates as intended in the infrared, successful characterization of a commercial detector designed to operate in the 8-12 micron range would more satisfactorily validate this system and is being conducted as follow-on research.

1150 Kelvin Blackbody Exitance
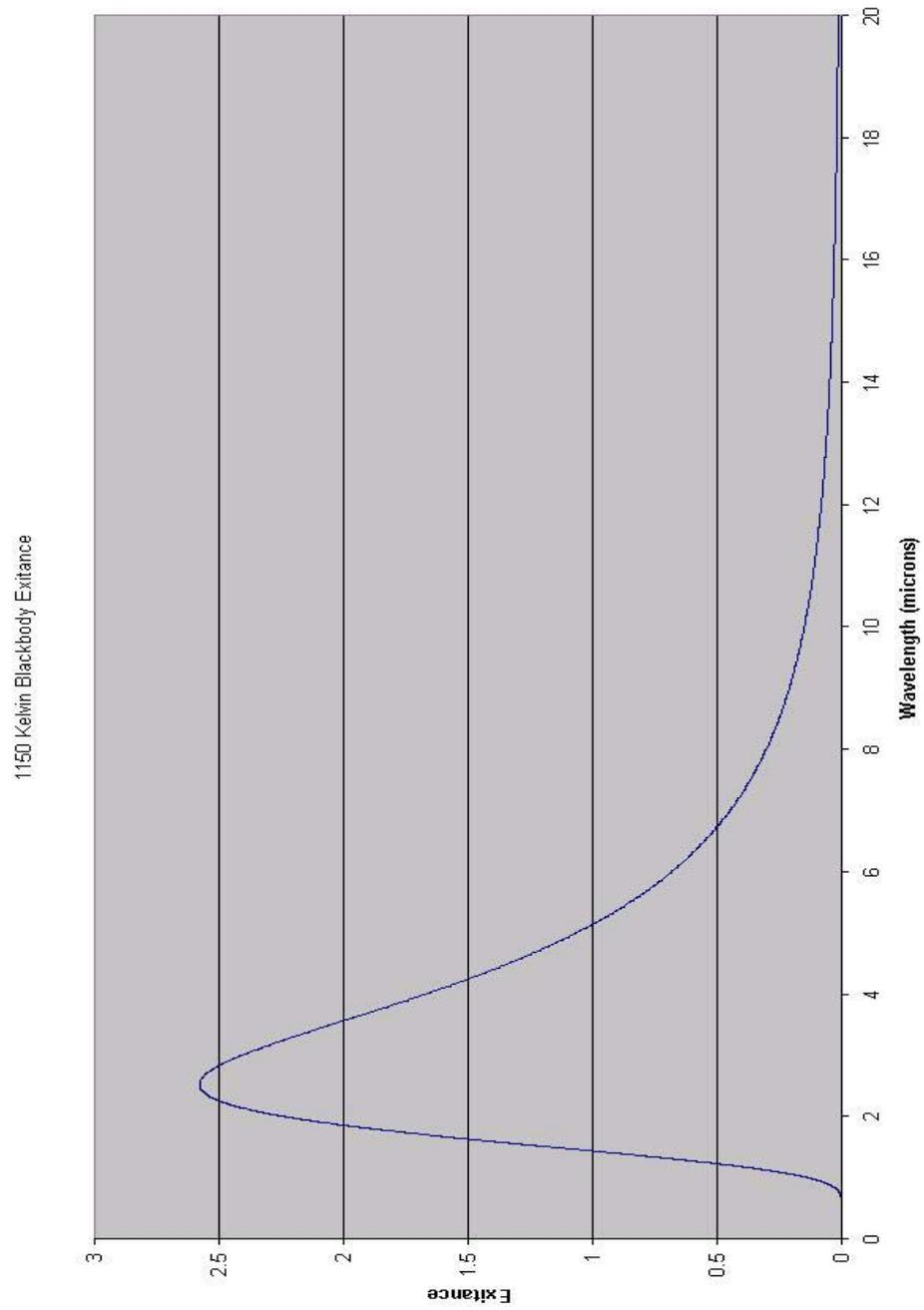
Figure 20.   Blackbody Radiation Curve for a 1150 Kelvin Source
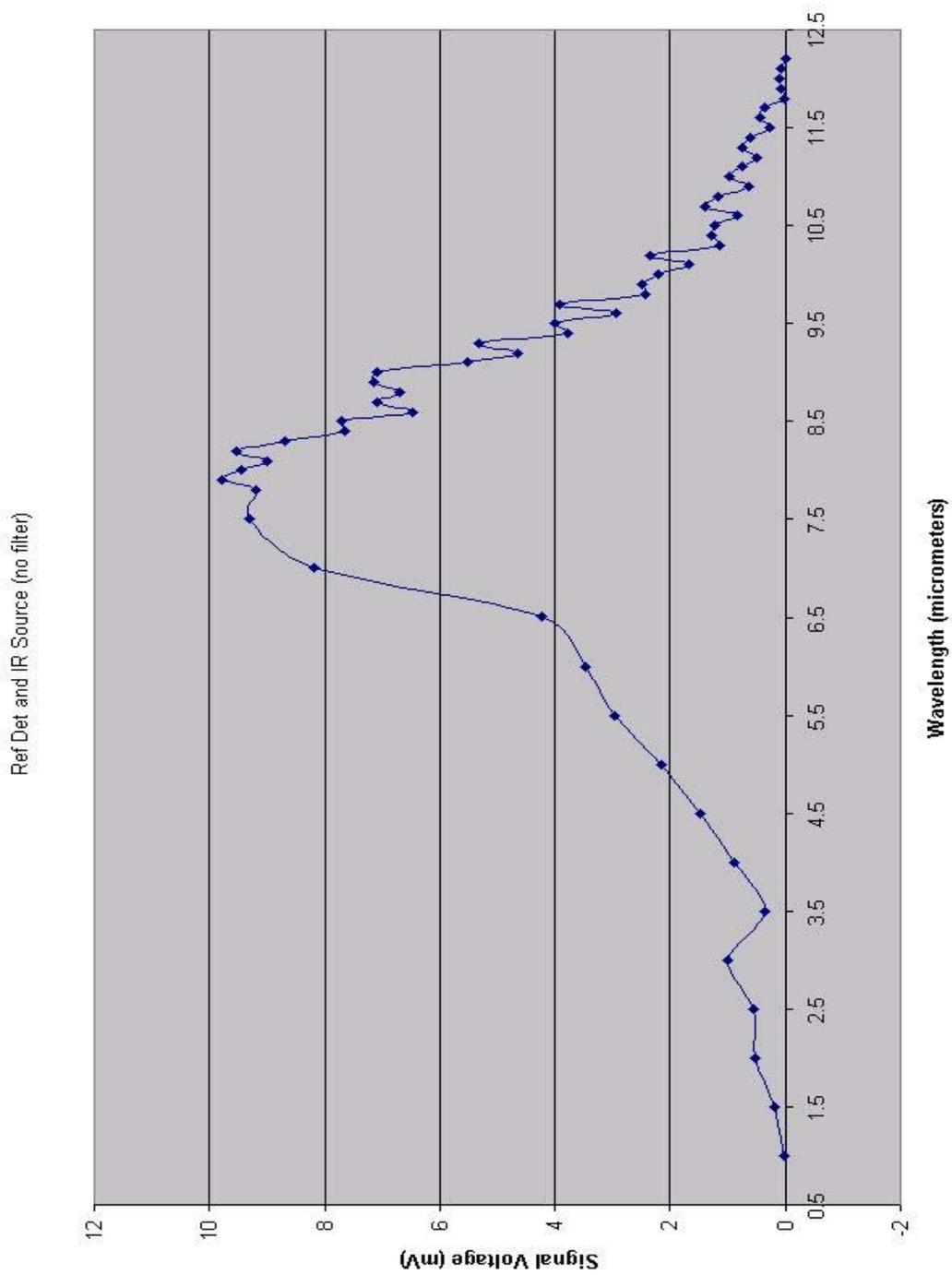
Figure 21.   Reference Detector IR Response (7 micron blaze grating; no filter installed)
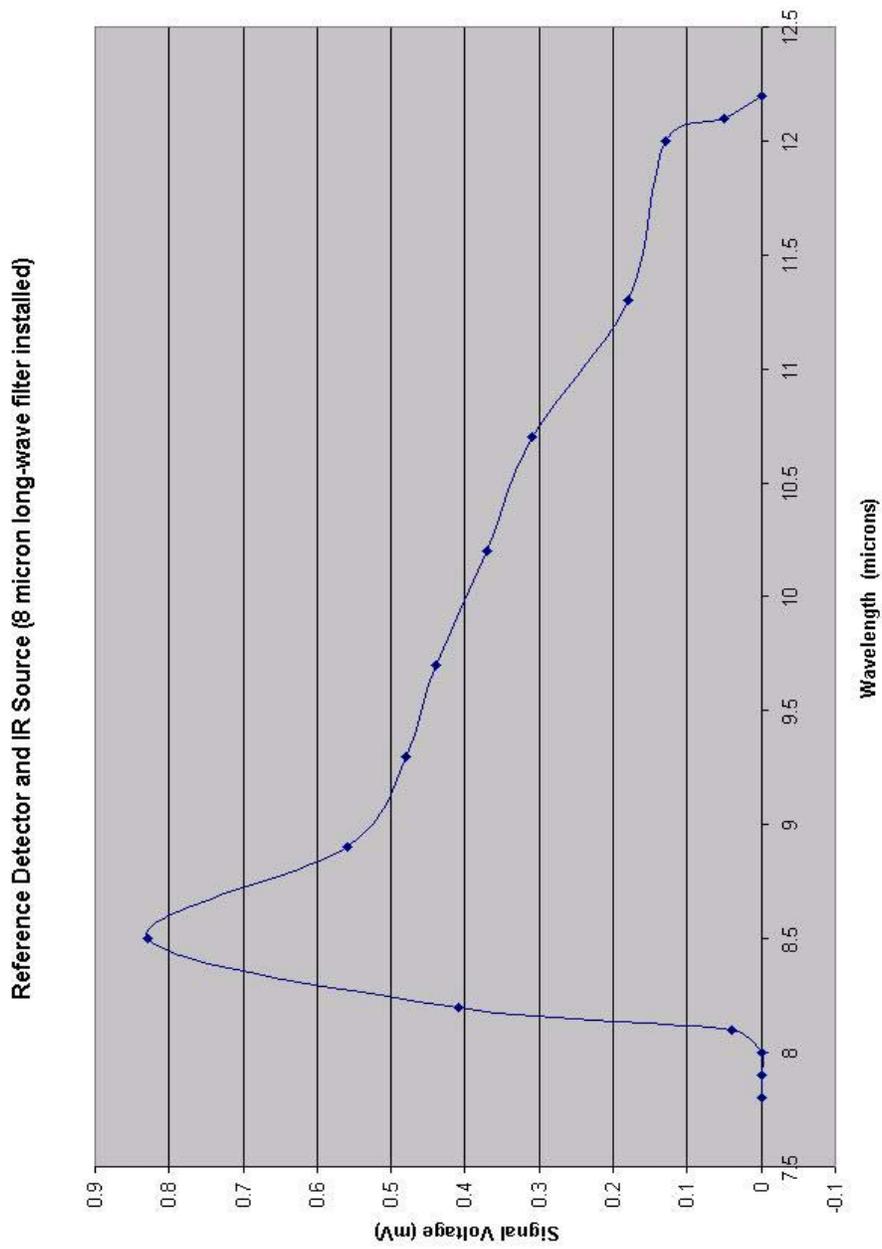
Figure 22.   Reference Detector IR Response (8 micron filter installed)

While the evaluation depicted in Figures 20 through 22 clearly demonstrates that the system is operating as intended, it also demonstrates the limitations of the system for applications in the 3-5 micron range (e.g. evaluation of an InSb device) where the grating serves to attenuate radiation below a useful level. Use of the 1000 nm blaze grating would result in similar attenuation, although it would be from the upper limit of its operating bandwidth rather than the lower limit (as is the case with the 7000 nm blaze grating depicted in this evaluation). Installation of the appropriate filters and grating identified earlier (and corresponding changes to the PCS VI) may be incorporated to optimize the system for operation in the 3-5 micron range.

V. OPERATING GUIDELINES

A. CAUTIONS

1. Switching Between the IR Element and QTH Lamp

Since the IR element operates at up to 12.8 amps, and the maximum operating current for the QTH lamp is 8.3 amps, damage to the QTH lamp can occur if the power supply is not set to zero amps following use of the IR element. The following sequence should be followed when switching between the two elements in the monochromator illuminator.

a. Rotate the locking ring counterclockwise to free the control knob.

c. Rotate the control knob counterclockwise to the stop; ensure 0 Amps displayed.

d. Turn the power supply OFF.

e. Connect the new lamp to the power supply.

f. Turn the power supply ON.

g. Slowly increase the current to the appropriate value for the new lamp.

h. Rotate the locking ring clockwise to lock the control knob.

i. For the IR element, allow a minimum of 30 minutes for thermal stabilization.

2. Handling of Optical Components

Body oils and dust pose the greatest threat to the performance and longevity of optical components. Therefore, when handling gratings, mirrors and lamps, ensure that protective gloves (e.g. Ansell Edmont Industrial "Poly-D" disposable polyethylene gloves, or similar) are worn. Additionally, dust and debris, which may accumulate on optical components, should only be removed with compressed nitrogen specifically packaged for that purpose. The first burst of compressed nitrogen should be directed away from the optics to ensure that any moisture or debris that may collect in the spray nozzle are not ejected onto the surface that is to be cleaned.

3.   Changing Lock-In Amplifier Voltage Scales (Sub-VI Alteration)

Caution should be exercised if a decision is made to alter the voltage scale on the lock-in amplifier sub-VI.   Data processing is conducted with voltage in millivolts; therefore only millivolt scales should be selected for display. *No adjustment should be necessary*, however, since the faceplate displays of the amplifier itself are unreliable during a scan. Accurate readouts for detector voltages are provided on the front panel of the PCS VI (computer screen).

B.   SETUP

To operate the system, first, turn on all of the equipment and remove the dust covers from the optics. Occasionally, communication errors between the computer and the monochromator can occur if the computer is on-line before the monochromator has completed its internal checks and "checked-in". Therefore, having the computer up and running prior to powering up the other equipment is recommended. Open LabVIEW from the Windows Start menu under Programs. Select "Open VI", then locate the PCS VI and select it. Once the PCS VI has been opened, select the Window pull-down menu and select "Show Diagram". This will afford the operator greater control over the VI while it is running. Finally, the schedule for the diffraction gratings and filters must be entered (or verified) prior to using the system. These procedures can only be accomplished while the VI is running -- specific instructions follow.

1.   Setting (checking) the Grating Schedule

The PCS VI allows the operator to identify the band of wavelengths for which each grating in the monochromator will be used. The software assumes that the three gratings will be used sequentially. Fixed values of 0 and infinity (Inf.) define the beginning and ending limits of the wavelength band. The two remaining transition wavelengths are open for operator modification. Operating limits for each grating may be obtained from their performance specifications. To alter the wavelength values for grating transitions, follow these steps:

a. Open the PCS VI and select RUN (the small white arrow at upper left).

b. Depress the button marked Grating to open the window for these parameters.

c. Enter the transition wavelengths and close the window.

d. Select "Operate" from the pull-down menus.

e. Select "Make current values default".

f. Close the VI (unless additional work is to be conducted).

2.   **Setting (checking) the Filter Schedule**

The PCS VI allows the operator to identify the band of wavelengths for which each filter in the filter wheel will be used. The software assumes that the six filters will be used sequentially. Fixed values of 0 and infinity (Inf.) define the beginning and ending limits of the wavelength band. The five remaining transition wavelengths are open for operator modification. Keep in mind that the effective operating band for any long-wavelength filter exists from the cut-on wavelength of the filter to twice that cut-on wavelength. To change the filter change-over points, follow these steps:

a. Open the PCS VI and select RUN (the small white arrow at upper left).

b. Depress the button marked Filter to open the window for these parameters.

c. Enter the transition wavelengths and close the window.

d. Select "Operate" from the pull-down menus.

e. Select "Make current values default".

f. Close the VI (unless additional work is to be conducted).

3.   **Mechanical Alignment**

Verify the mechanical alignment of the components. Operating the monochromator with the wavelength set to zero will provide a maximum-intensity, visual image (QTH lamp operating) to support initial alignment. Following visual alignment, reference the voltage displayed on the respective lock-in amplifiers to fine-tune the

alignment and focusing of the beams on the detectors. Ideally, this procedure should be completed prior to each data collection run with the equipment (at a minimum, after detectors or changed or components are repositioned).

C.   DATA COLLECTION

1.   Executing a Scan

Once the filter and grating schedules have been stored in the PCS VI, the remaining features of the front panel are tailored to driving the monochromator to a particular wavelength (e.g. the "GoTo" command) or executing a sweep of wavelengths in accordance with scan parameters provided by the operator (e.g. "Go Scan"). To execute a scan, follow the steps below:

a. Enter the first wavelength in the sequence into the "GoTo" window.

b. Drive the monochromator to the first wavelength by pressing "GoTo".

c. Enter values for: Start Wavelength, End Wavelength and Step Wavelength.

d. Selecting a delay / dwell time of 1 second.

e. Press "GoScan".

Note: During the first scan for a given set of parameters, the graphic displays on the front panel will default to an initial data point at zero wavelength which can skew both the x and y axes of the plots and generate a line from the origin to the first data point. If a need exists to print the screen, and only the wavelengths within the commanded scan are desired for display, this can be achieved in the following manner:

a. Select "Go Scan".

b. After the scan has begun, select "Stop Scan".

c. Execute a second scan following the procedures outlined above.

2.   Exporting Data to a Spreadsheet Compatible File

Once a scan has completed or been interrupted, the PCS VI presents a pane that prompts the operator to identify a file name and destination for exporting of the data that has been collected. The output format is a delimited text file that is compatible with spreadsheet software such as Microsoft Excel and Lotus 1-2-3. If no requirement for data storage exists, then the operator may select "Cancel". If the file export is canceled, then the operator may elect to "Continue" (which returns the operator to the control panel for another scan or other operations), or to "Stop" (which exits the RUN mode of the VI). Data is output in five columns arranged as shown in Table 6, below. Headings are not provided in the delimited text file, so this table is key to interpreting the data.

Table 6.   File Output (Column Headings).

Index	Voltage (ref. detector)	Voltage (sample)	Wavelength (nanometers)	Responsivity (amps / watt)

3.   Stopping a Scan In-Progress

Selecting "Stop Scan" from the front panel will halt the scan in progress, but not before the following sample-hold-average cycle has completed. A more direct method of stopping execution is available, *but does not provide the option to store the existing data to a file*. By opening the diagram window prior to running the PCS VI, the stop button in the tool bar of the diagram window can be used to immediately halt execution and exit the run mode. If the diagram window is not opened prior to starting a scan, it cannot be opened while the VI is running and only the "Stop Scan" option is available to the operator.

Note: The "Exit" button on the front panel is inoperative during a scan, but can be used to leave the LabVIEW environment entirely during the run mode under any other circumstance.

THIS PAGE INTENTIONALLY LEFT BLANK

VI. CONCLUSIONS AND RECOMMENDATIONS

This photodetector characterization system (PCS) was constructed for the evaluation of "dual-color" (1 μm and 8-12 μm) Quantum Well Infrared Photodetectors (QWIPs); specifically, to validate QWIP design algorithms developed under parallel research efforts and to verify device performance in accordance with design specifications. The system was designed to support expanded modes of operation, and the system may be used to characterize the response of detectors that operate anywhere within the band from 600 nm to 16 μm. A manual transition between source elements is required at approximately 2 μm due to the spectral bandwidth of each. Evaluations within the spectrum of either source are fully automated.

This system has satisfactorily characterizes a photodetector of known performance specifications (e.g. Silicon) and is considered suitable for use as a test instrument for future evaluations at near-infrared wavelengths (1 micron). Although the system meets design criteria for operation at infrared wavelengths, successful characterization of a commercial detector designed to operate in the 8-12 micron range would more completely validate this system. The system is well suited to follow-on development as the software is well commented and may be easily tailored for future applications. The only present operational restriction on the system is that evaluation of responsivity at wavelengths below approximately 600 nm is precluded in the current configuration. This limitation may be easily corrected through installation of a different reference detector and some minor software modifications.

Evaluation of additional detectors of known response characteristics will greatly increase the proficiency of operators and instill greater confidence in the system. Ideally, a set of commercial detectors that cover the entire operating spectrum of the system should be assembled. Ready access to such devices would support academic demonstrations, further system development, and accurate calibration. Consideration should be given to augmenting the Silicon detector already in use with detectors such as Mercury Cadmium Telluride (HgCdTe; or "MCT"; operation to as high as 13 microns),

Germanium (Ge; 1-1.8 micron range) and/or Indium Antimonide (InSb; 1-5 micron range).

Finally, while the system operates quite well for the intended application, some software tailoring may be required to optimize performance for other applications. Therefore it is highly recommended that one or more individuals maintain a working knowledge of the software and proficiency in LabVIEW programming.

APPENDIX I : COMPONENTS & SPECIFICATION SHEETS

A.   PCS PARTS LIST (PAGE 1 OF 2)

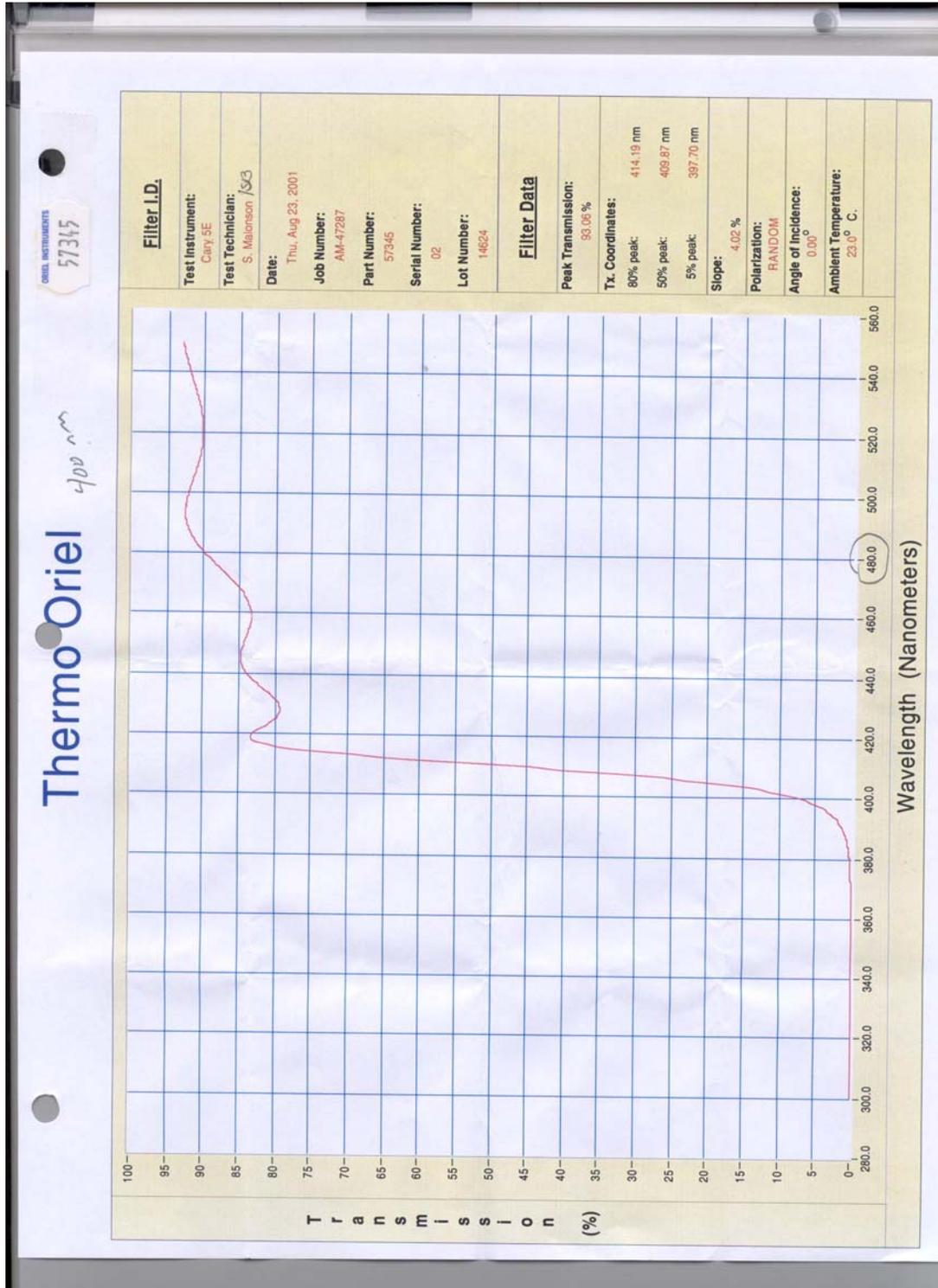| Part No.	Quantity	Cost ($CY02)	Description (purpose)
3501	1	NPS on-hand	**Optical Chopper (wheel and controller)** Brand / Vendor: New Focus (modulation of energy; supports signal processing)
**	**	**	***
5210	2	NPS on-hand	**Lock-In Amplifiers** Brand / Vendor: EG&G Princeton Applied Research
**	**	**	***
74112	1	$6731	**CS 260 Monochromator** (source / generates desired wavelength)
74001	2	Incl #74112	**Micrometer Driven Slit Assembly** (controls aperture in/out of CS260)
74066	1	Incl #74112	**Diffraction Grating** 600L/mm 400nm blaze
74067	1	Incl #74112	**Diffraction Grating** 600L/mm 1000nm blaze
74082	1	Incl #74112	**Diffraction Grating** 75L/mm 7000nm blaze
**	**	**	***
7340	1	$1762	**Manual Monochromator Illuminator** (twin-lamp source assembly)
6333	1	$50	**100 Watt QTH lamp** (quartz-tungsten-halogen source)
73902	1	$576	**Lamp Mount Assembly for 6333**
6363	1	$380	**IR Emitter (a.k.a. "glow bar")**
73906	1	$605	**Lamp Mount Assembly for 6363**
63938	1	$1347	**Power supply for 6333 / 6363**
**	**	**	***
74010	1	$1036	**Motorized Filter Wheel** (six filters, reduces high-order "noise")
57345	1	$155	**VIS / NIR Long Pass Filter** (400nm / 1-inch diameter)
57353	1	$155	**VIS / NIR Long Pass Filter** (600nm / 1-inch diameter)
57369	1	$155	**VIS / NIR Long Pass Filter** (1000nm / 1-inch diameter)
57955	1	$155	**8.0 micron IR Long Pass Filter**
**	**	**	***
74102	1	$556	**Baseplate** (fixed mount for CS260, Illuminator & Filter Wheel)

All parts from ThermoOriel unless otherwise noted
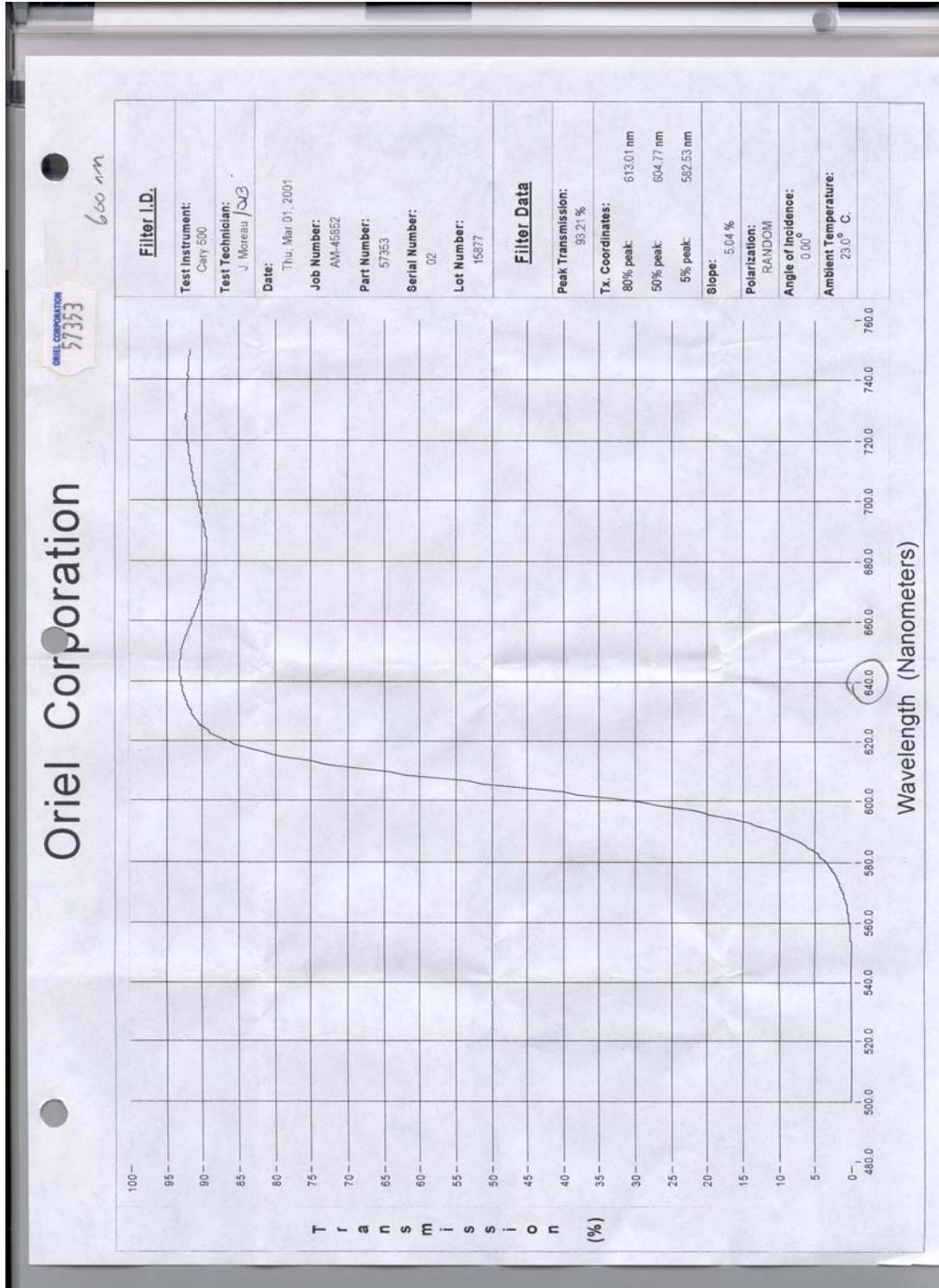
B.   PCS PARTS LIST (PAGE 2 OF 2)

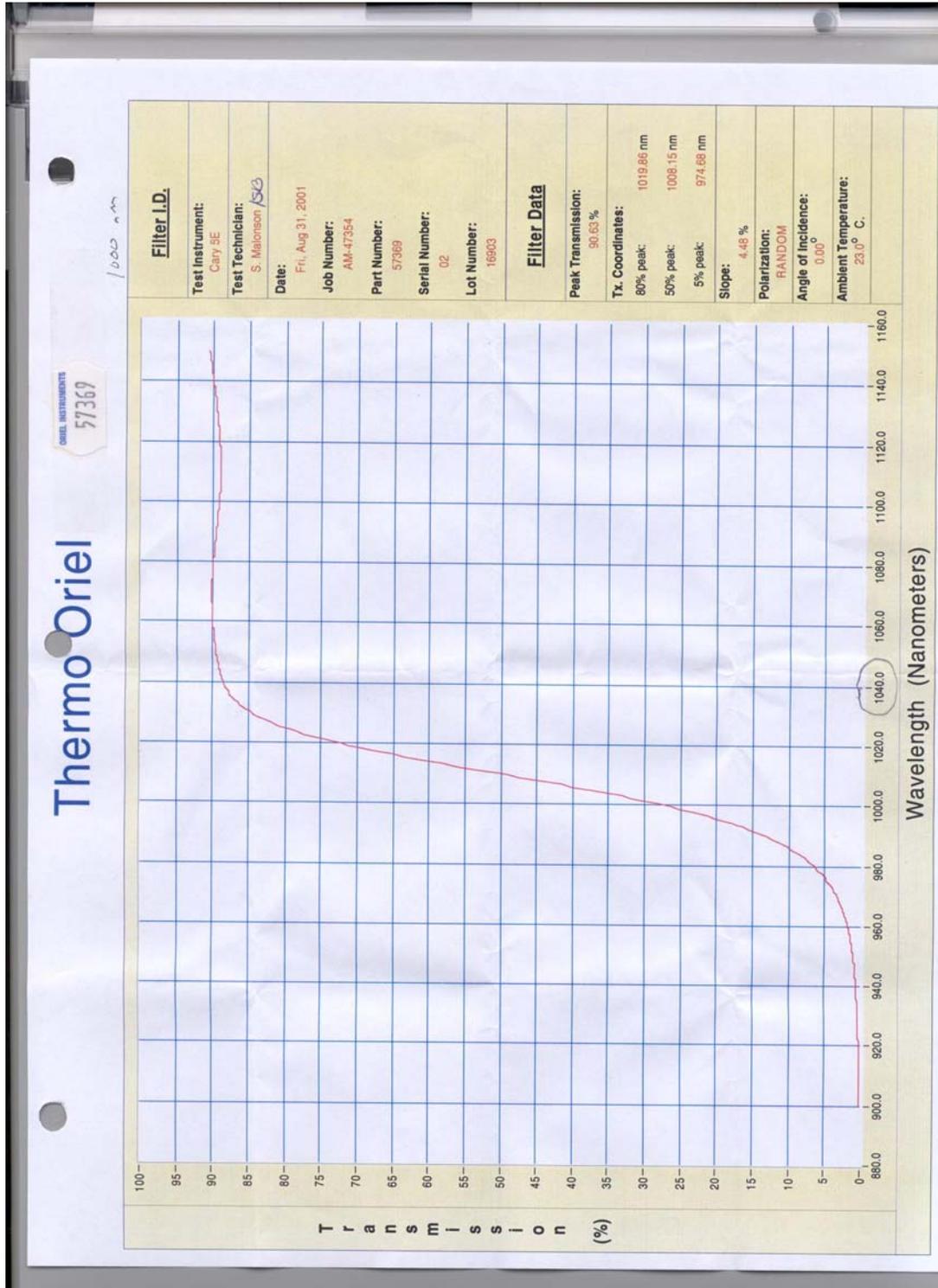| Part No.	Quantity	Cost ($CY02)	Description (purpose)
8104001	1	on-hand	**Detector Refrigeration Assembly** Model 22, Serial No. 11B019989 CTI – Cryogenics Helix Technology Corporation
11601	2	$152 ea	**Universal Carrier, Large** (sliding mounts for sample refrig. assy.)
11512	1	$267	**Large Table Rail – 24 inch** (track for sliding mounts)
**	**	**	***
70124	1	$1134	**Pyroelectric Detector Head** (reference detector; flat response curve)
12401	1	$283	**Damped Optical Rod** (support reference detector)
14295	1	$508	**Rod Slide, fine adjustment** (support reference detector)
12352	1	$24	**Rod, Std 10.2-inch** (course mounting arrangement for reference detector)
14423	2	$39	**Rod Holder, Std 6-inch** (coarse mounting arrangement for reference detector)
**	**	**	***
38111	1	$357	**Beam Splitter, Grating, 60-degree** (splits energy 50/50 to two detectors)
14004	1	$92	**Mini-mount** (for 38111 beam splitter)
**	**	**	***
45347	3	$584	**Off-Axis Paraboloidal Ref. Mirror** (directs beam from source to detectors)
45357	3	$60	**Mounting Disk for Paraboloidal Ref Mirrors** (supports mounting with ¼-20 thread hardware)
12051	3	$215	**Tilt Tables** (fine control of paraboloidal ref. mirrors)
**	**	**	***
11655	6	$69	**Moveable Holes** (allows for movement of rod-mounts on table)
12510	6	$13	**Rod Collars, Std.** (fixes optical height of rod-mounted devices)
14422	4	$35	**Rod Holders, Std 3-inch**
12312	5	$13	**Rod, Std 1.5-inch**
14280	5	$38	**90-degree rod connector** (orients rods parallel to table)
12332	5	$21	**Rod, Std 4-inch**
16121	1	$336	**Horizontal Translator**

All parts from ThermoOriel unless otherwise noted

C.   400 NANOMETER FILTER (#57345)

D.   600 NANOMETER FILTER (#57353)

E. 1 MICRON FILTER (#57369)

F. 8 MICRON FILTER (#57955)

Date: 2001-05-23 07:41

Operator : /S

Filter specification :
LP (Longwavepass)

Cuton 5% = 8000 +/- 150 nm
Blocking : UV nm
Slope : 5 %

Size : 25,4x1,0 mm

Qty : 3 pcs

Art.nr : 713
Batch nr :
Order nr : 01.107 34/ S-105-350

Customer
Part nr : 579 55
P.O. nr : 499 66

"8 μM LONG-PASS"

P-E FTIR Optica 2000

cm-1

Diagram range : 1400 to 651,5 cm-1

Data collection range : 1400 to 600 cm-1   Slope : 1,52 %

Actual sample values :

Cuton 5% = 8059,3 nm (1240,8 cm-1) OK
HP = 8152,6 nm (1226,6 cm-1)
Tmin. = 53,8 %
Tmax. = 92,9 %
Tave. = 85 %
T-range : 8183 to 16639 nm (1222 to 601 cm-1)
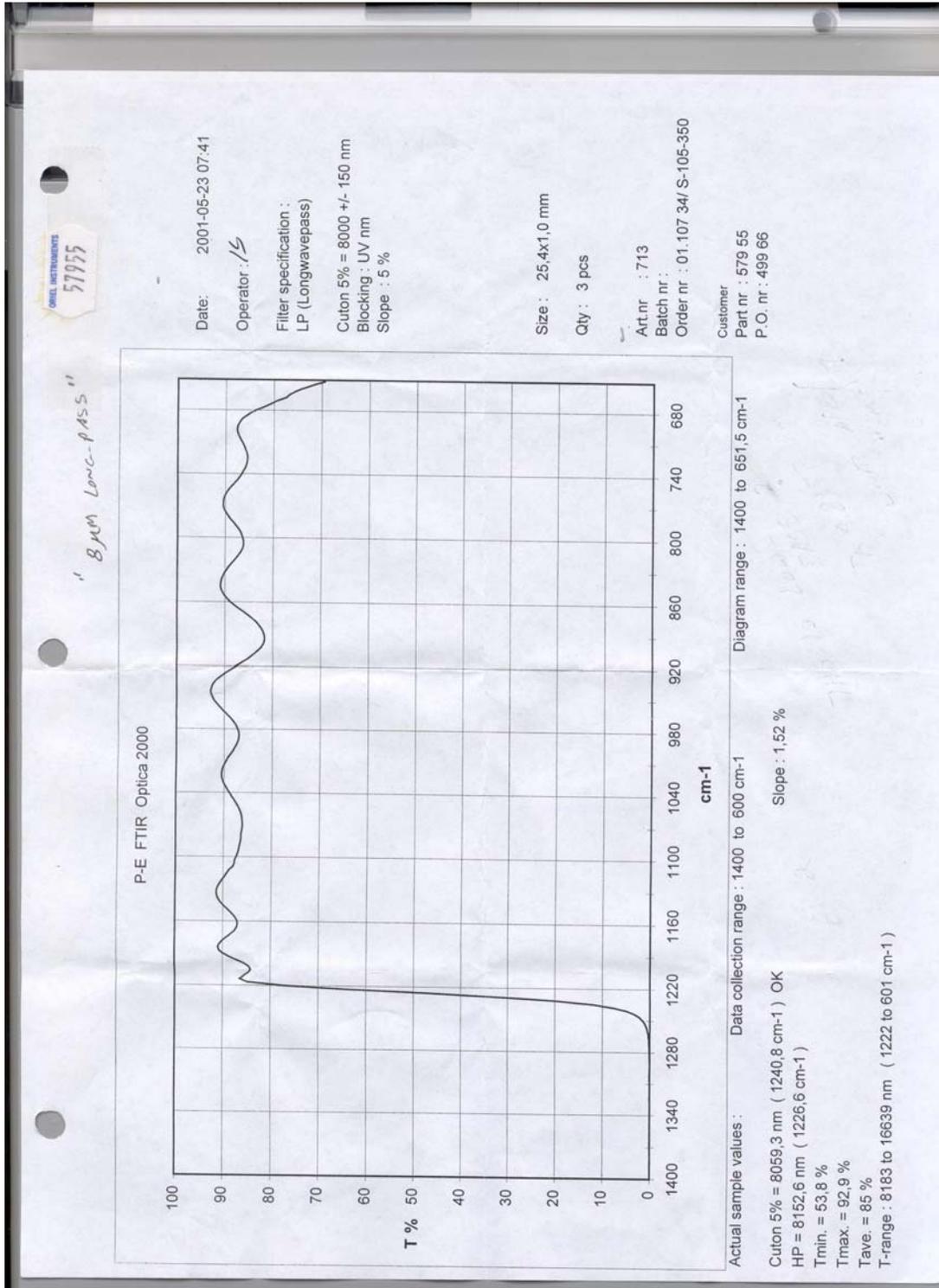
G.   REFERENCE DETECTOR (SHEET 1 OF 2)

Two Active Areas and Two Windows Types

We offer detector heads with 2 mm or 5 mm diameter detector active area and windows of either Thallium Bromoiodide (KRS-5) of Calcium Fluoride (CaF_2). KRS-5 covers wavelengths from 0.6 to 50 micrometer, and CaF_2 covers 0.45 to 9 micrometers. Both detectors include a compensating preamplifier and both are carefully calibrated.

- The 70128/70364 and 70129/70365 have 2 mm diameter area useful for many laser or focused beam applications.
- The 70123/70362 and 70124/70363 have a 5 mm diameter detector element. The large area makes this detector useful for monitoring the output of monochromators or for applications where it is not possible to focus the radiation tightly.
- The 70123/70362 and 70128/70364 have CaF_2 windows.
- The 70124/70363 and 70129/70635 have KRS-5 windows.

Both detectors have oversize windows to prevent vignetting at high F numbers. However, some fall off of radiant energy will occur as the angle of incidence of radiation falling on the detector window gets more shallow (reflection losses increase with decreasing angles to the window surface).

Lithium Tantalate Elements

These detectors use lithium tantalate crystals in sealed housings to minimize the effects of air currents, humidity, ambient temperature and to provide long term stability. The crystals have a proprietary black coating to enhance the responsivity and minimize spectral response variations. The relative response of the blackened elements is essentially flat from below 0.2 micrometer to beyond 30 micrometers. The window material limits the spectral extent the responsivity. See Figure 2 for relative responsivities of the detector, CaF_2 and KRS-5.

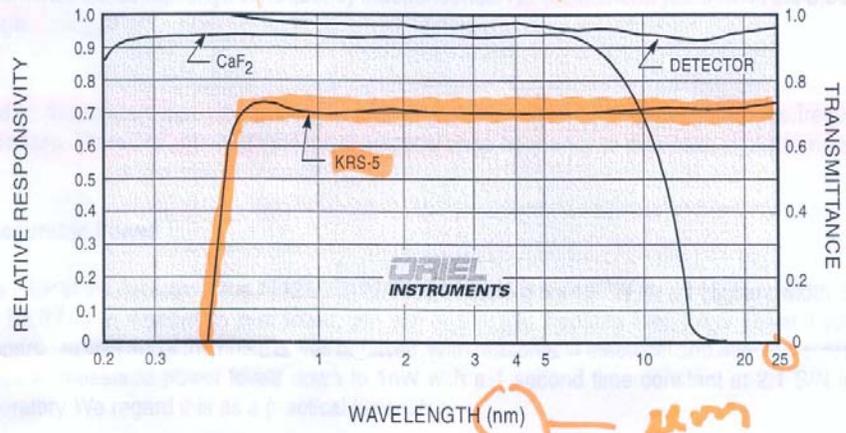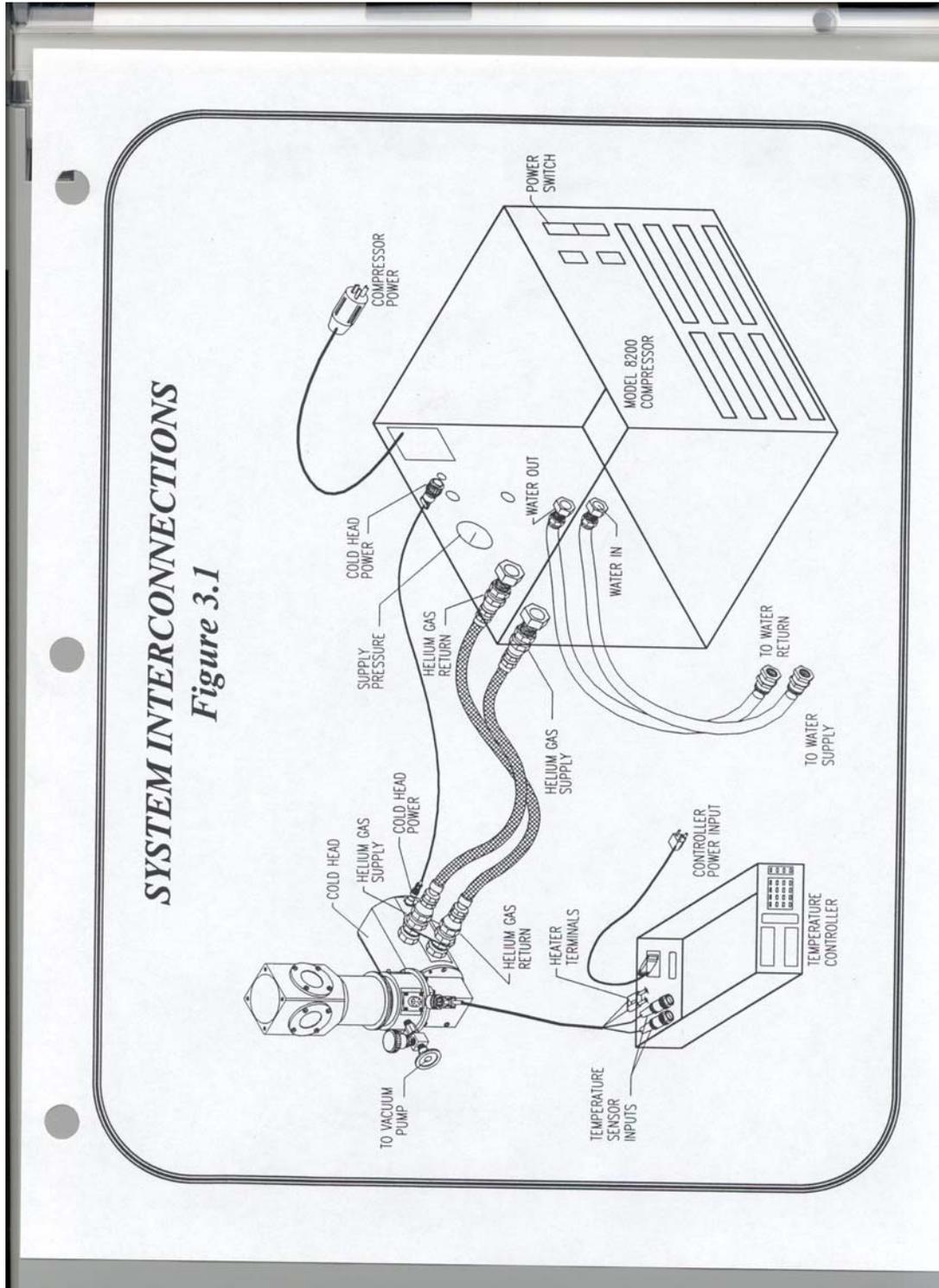## H.   REFERENCE DETECTOR (SHEET 2 OF 2)

Fig. 2 Relative spectral response of blackened Lithium Tantalate detectors and transmission of KRS 5 and CaF₂ Windows

I. CLOSED LOOP REFRIGERATION SYSTEM (SHEET 1 OF 2)

SYSTEM INTERCONNECTIONS
Figure 3.1

61

SYSTEM ACCESS
Figure 4.1

- 1/4-20 TAPPED MOUNTING HOLES
- VACUUM SHROUD
- VACUUM FLANGE
- RADIATION SHIELD
- RADIATION SHIELD MOUNTING SCREWS
- SAMPLE HOLDER
- SAMPLE MOUNT
- EVACUATION VALVE OPERATOR KNOB
- VACUUM FLANGE
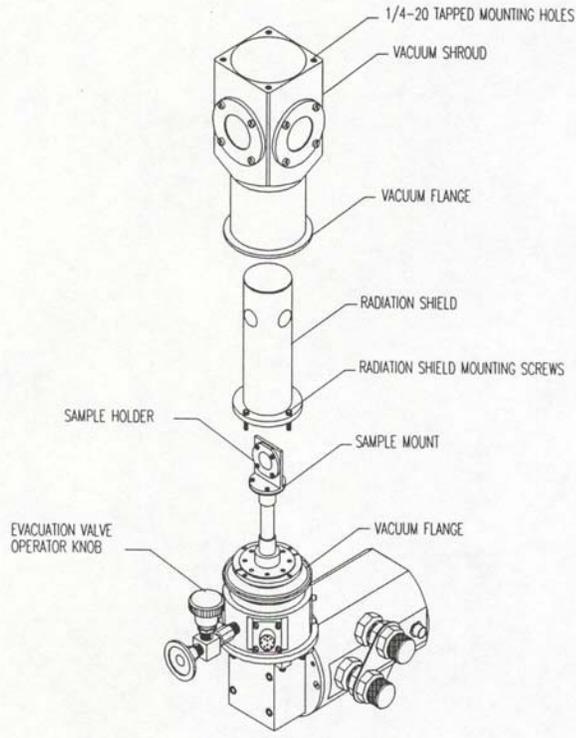
APPENDIX II : POINTS OF CONTACT

A.   **THERMO ORIEL**

180 Long Beach Boulevard

Stratford, CT, 06615-0872

(203) 377-8282

www.oriel.com

POC: Donna Rawson (drawson@oriel.com)

B.   **NATIONAL INSTRUMENTS (LABVIEW)**

1350 Terra Bella Ave.

Mountain View, CA, 94043

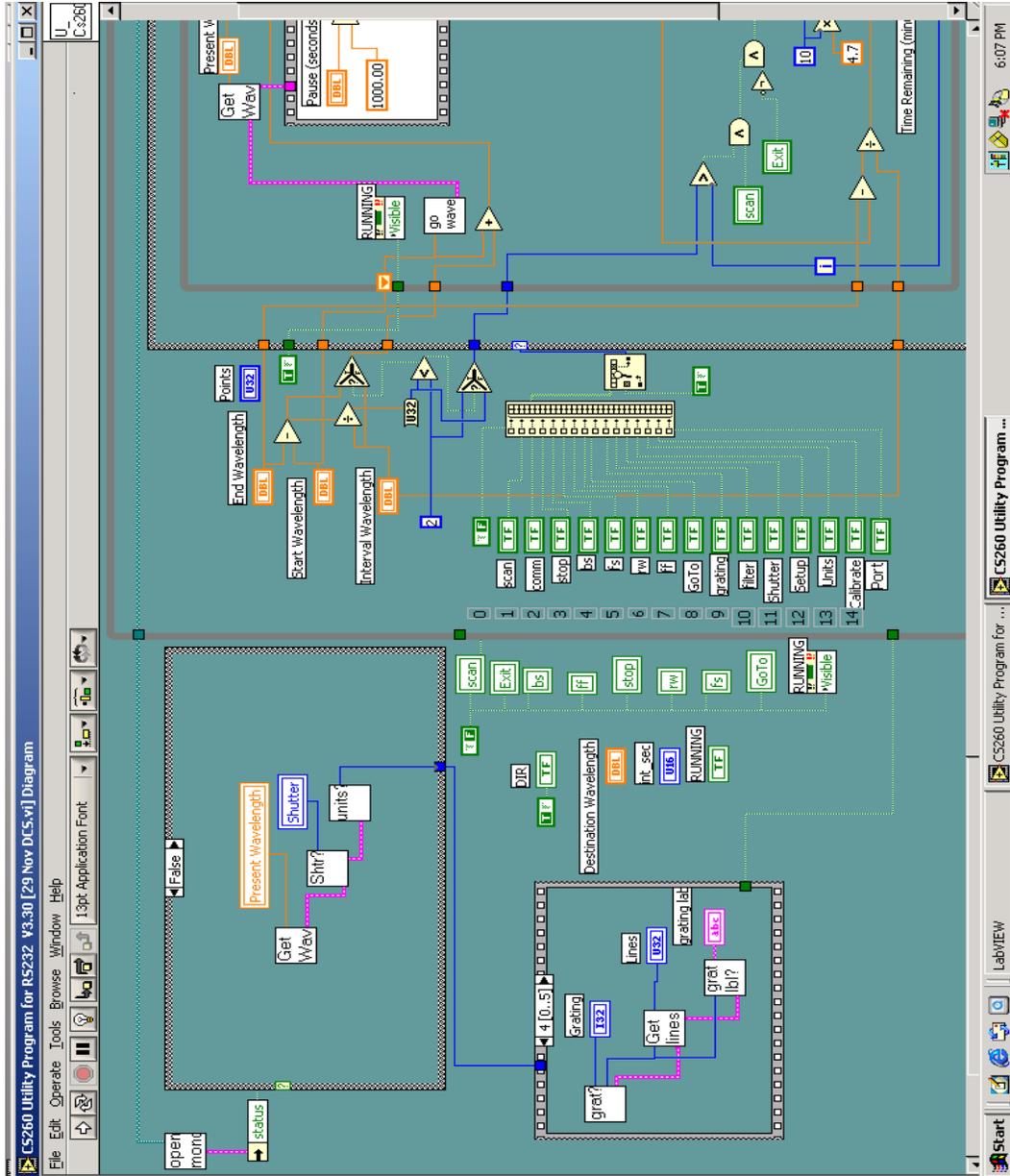(800) 433-3488

www.ni.com

POC: Sue Park, Field Sales Engineer, (650) 934-0547

THIS PAGE INTENTIONALLY LEFT BLANK

# APPENDIX III: PROGRAMMING DOCUMENTATION

A. WIRING DIAGRAM (SCREEN CAPTURE; 1 OF 4)

Depicts interface for monochromator control (left two-thirds of frame) and case structures that comprise the "Go Scan" sequence.

Depicts left half of the "Go Scan" case structures. The logic structure in the lower left corner of the frame generates an estimate of time remaining in the scan. The middle block executes the sample / hold sequence, polling the lock-in amplifiers via sub-VIs during each execution. The right-most block accomplishes averaging of the data at completion of each sample / hold sequence using the "mean" sub-VI available from the LabVIEW development suite. Values passed to the next segment form "data points" and include average voltages from each detector and the wavelength associated with each.
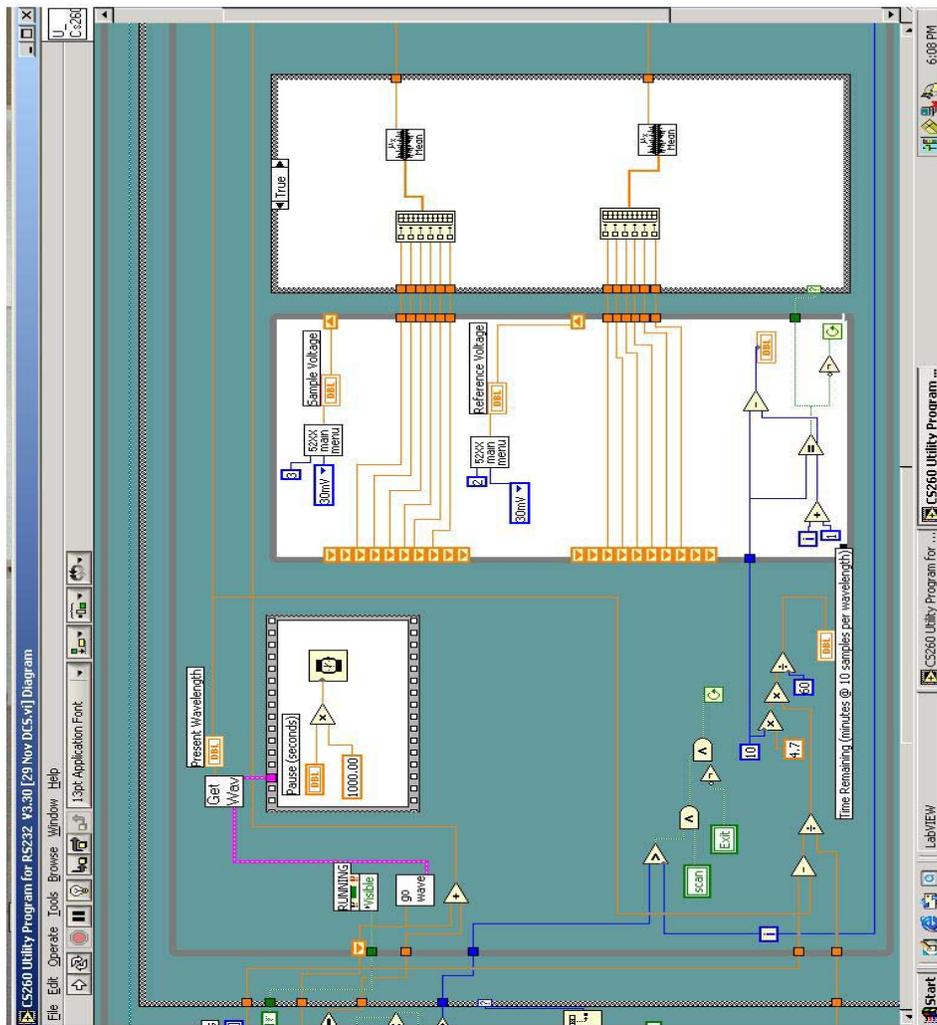
C. WIRING DIAGRAM (SCREEN CAPTURE; 3 OF 4)

The small block in the upper right of the frame is the array responsible for storing each data point as it is generated. The entire case structure for "Go Scan" is wavelength dependent, and all the functions contained therein execute exactly as FOR or WHILE loops would in line-by-line programming languages like FORTRAN or C++. This includes the complex at the lower right of this frame, which updates the graphic displays on the front panel.

D. WIRING DIAGRAM (SCREEN CAPTURE; 4 OF 4)

The three, large, nested case structures complete operation from the inside out (sequentially). Once all data is collected, it is passed to the file output sequence that is trapped between the inner case structure (data collection) and the next in the sequence ("Go Scan"). If the operator chooses not to send data to a file, and elects to "Close" from the file prompt window, operation shifts outside the largest case structure and the run mode is exited.

68

LIST OF REFERENCES

1. "SA-16 GIMLET Man-portable Surface-to-air Missile System";
http://hometown.aol.com/threatmstr/airdef.htm, 23:45 GMT, 2 December 2002

2. "Quantum-Well Infrared Photodetectors", B.F. Levine, AT&T Bell Laboratories, Murray Hill, N.J., 07974. Reprinted from the Journal of Applied Physics, Volume 74, Number 8, 15 October 1993.

3. Electronic Engineer's Handbook, 2nd Edition, Donald G. Fink and Donald Christiansen, McGraw Hill, Inc. 1982, ISBN 0-07-020981-2.

4. Fundamentals of Photonics, Bahaa E.A. Saleh and Malvin Carl Teich, John Wiley & Sons, Inc., 1991.

5. The Principles of Optics, Arthur C. Hardy and Fred H. Perrin, McGraw Hill Book Co., Inc., New York and London, 1932.

6. Introduction to Modern Optics, 2nd Edition, Grant R. Fowles, Holt, Rinehart & Winston, 1975, ISBN 0-03-089404-2.

7. The Book of Photon Tools, Oriel Instruments, Stratford, CT, 2001.   Note: no page numbers will accompany references to this document, as it is replaced regularly and the 2001 version will likely be unavailable very shortly after this document is completed. All components and topics are also available on-line at www.oriel.com. through their tutorials or online-catalog.

8. Infrared Detectors and Systems, E.L. Dereniak and G.D. Boreman, John Wiley & Sons, Inc., New York, 1996, ISBN 0-471-12209-2

9. "Getting Light Into a Monochromator", A Tutorial, Oriel Instruments, http://www.oriel.com/down/pdf/04006.pdf, 00:31 GMT, 3 December 2002

10.   National Instruments website at: http://amp.ni.com/niwc/labview/lv.jsp, 02:05 GMT, 3 December 2002. See also http://www.ni.com.

THIS PAGE INTENTIONALLY LEFT BLANK

INITIAL DISTRIBUTION LIST

1.   Defense Technical Information Center
      Ft. Belvoir, VA

2.   Dudley Knox Library
      Naval Postgraduate School
      Monterey, CA

3.   Dr. Ike Bendall
      SPAWAR (Bayside)
      San Diego, CA

4.   Professor Gamani Karunasiri
      Naval Postgraduate School
      Monterey, CA

5.   Professor Scott Davis
      Naval Postgraduate School
      Monterey, CA

6.   Professor William R. Maier II
      Naval Postgraduate School
      Monterey, CA